ACTA NEUROBIOLOGIAE EXPERIMENTALIS

Acta Neurobiol. Exp. 1997, 57: 289-314

Diversity of connections of the temporal neocortex with amygdaloid nuclei in the dog (*Canis familiaris*)

Anna Kosmal, Monika Malinowska and **Agnieszka Woźnicka**

Department of Neurophysiology, Nencki Institute of Experimental Biology, 3 Pasteur St., 02-093, Warsaw, Poland, Email: aka@nencki.gov.pl

Abstract. Reciprocal connections of amygdaloid nuclei with the temporal neocortex in the dog were investigated. Injections of fluorescent tracers and BDA into particular temporal areas were made in eleven dogs. The topographical arrangement of connections and variations in their density differentiate the temporal neocortex in the dog into a few regions. Among them, the cortex involving the anterior part of the ectosylvian gyrus did not send any amygdalopetal projection. The middle ectosylvian, dorsal zone of the posterior ectosylvian and the anterior part of the Sylvian gyrus were weakly connected with the amygdala. The cortical region involving the ventral zone of the posterior ectosylvian and composite posterior areas, as well as posterior Sylvian gyrus, was characterized by profuse connections with the amygdaloid complex. Cortico-amygdaloid connections originate in the wide cortical area of the auditory cortex of the middle and dorsal part of the posterior ectosylvian gyrus as well as in the auditory association cortex located in the ventral ectosylvian, composite posterior and posterior Sylvian gyri. The connections showed a dorso-ventral gradient of increasing density, in the direction of association fields. The most substantial projection taking rise from the ectosylvian posterior and posterior composite gyri terminated preferentially in the pericapsular sector of the lateral amygdaloid nucleus and, to a lesser degree, in its medial sector. Terminals of connections originating in the Sylvian gyrus occupied preferentially the intermediate part of the lateral nucleus, slightly more medially than that from the ectosylvian and posterior composite areas. Additionally, axonal terminals derived from the composite posterior and Sylvian posterior areas were observed in the basal parvocellular and magnocellular nuclei. Neocortical projections were reciprocated by amygdalofugal connections with two exceptions: the basal magnocellular nucleus was distinguished by a substantial amygdalofugal projection to the temporal neocortex focused on the dorsal Sylvian gyrus, and the central nucleus of the amygdala, in contrast, received an exclusively corticofugal projection.

Key words: temporal neocortex, amygdaloid connections, dog, fluorochrome dyes, BDA

INTRODUCTION

The cortico-amygdaloid connections provide an important route by which sensory temporal cortices may influence motivational and emotional behavior (Aggleton and Mishkin 1986, LeDoux 1992, Aggleton 1993), as well as cognitive and memory processes (Kesner 1992, Murray 1992, Rolls 1992). It has been found that amygdalopetal projections in primates originate from the association cortices of various modalities rather than from the primary sensory cortex (Turner et al. 1980, Amaral et al. 1992). Amygdalopetal projections were derived from higher order association areas of visual and auditory modalities, situated in the inferior and superior temporal gyrus as well as from the polymodal fields of the temporal pole and superior temporal sulcus (Markowitsch et al. 1985, Iwai and Yukie 1987, Baizer et al. 1993, Kosmal et al. 1997).

In nonprimates, the temporal neocortex seems to be predominantly related to the auditory modality, and its association fields were recognized as a source of a substantial amygdalopetal projection. In the rat, the "core" temporal field, which receives specific auditory information through the ventral nucleus of the medial geniculate body (Romanski and LeDoux 1993a), does not form a direct projection to the amygdaloid complex, whereas the cortical fields located around the core cortex were identified as a source of differentiated amygdalopetal projections (Mascagni et al. 1993, Romanski and LeDoux 1993b). It was further found that the projections terminate in the lateral amygdaloid nucleus. The dorsal part of the nucleus was preferentially related to the input of auditory information (Romanski and LeDoux 1993b). Similarly, the cortico-amygdaloid connections in the cat are derived from neurons located outside the primary auditory cortex, in the posterior Sylvian and posterior ectosylvian gyri. Their axonal terminals were observed in the lateral (Russchen 1982, Shinonaga et al. 1994) and central lateral amygdaloid nuclei (Russchen 1982).

The temporal neocortex in the dog involves a large extent of neocortex situated in the ectosylvian, Sylvian and posterior composite gyri. In the dog, like in the cat and rat, all of this cortex was considered to be related to the auditory modality. Early studies by Tunturi in the dog (1950, 1962) defined the ectosylvian gyrus as responsive to sound stimulation. Anteriorly, the border of the auditory cortex was delineated across the anterior part of the ectosylvian gyrus, whereas ventrally it was limited by the junction of the posterior ectosylvian and posterior composite gyri. Within the ectosylvian gyrus, anterior, middle and posterior areas were distinguished as differing in character of responses to sound stimulation. In the middle part of the gyrus, Tunturi defined the primary auditory cortex on the basis of specific responses to sounds of particular frequencies, with the lowest thresholds and shortest latencies. Using the Marchi technique, Tunturi (1970) found that lesions of the medial geniculate body caused anterograde degeneration of fibers reaching to the anterior and middle parts of the ectosylvian gyrus. Additionally, the Sylvian gyrus was included into the auditory cortex on the grounds of identification of retrogradely degenerated cells in the medial geniculate body following ablations of the gyrus (Sychowa 1963). In the dog, the posterior composite gyrus is a greatly enlarged region of neocortex, which continues dorsally onto the posterior ectosylvian gyrus, however, its morphofunctional attributes were not recognized until now. Previous studies of amygdalo - cortical connections, using the Nauta and Fink-Heimer methods, had demonstrated a prominent anterograde axonal degeneration, widely distributed to the temporal cortex (Kosmal 1976), however, their precise terminal topography and reciprocity were not defined.

The present study was undertaken in order to determine the organization of connections between particular fields of the temporal cortex and the amygdaloid nuclei using more sensitive methods related to axonal transport. We thus intend to provide more detailed information about the morphofunctional organization of the canine temporal neocortex.

METHODS

The housing, care and surgical procedures followed the guidelines established by the Ethical Committee on Animal Research of the Nencki Institute, based on a decree of the President of the Polish Republic.

Eleven adult mongrel dogs, weighing 10-12 kg, were used in this study. Three fluorochromes: 10% solution of fluoro ruby (FR, Fig. 1A,C), 3-5% solutions of fast blue (FB, Fig. 1B,D) and diamidine yellow (DY, Fig. 1B,E) as well as 10% solution of a recently introduced tracer, biotynylated dextran amine (BDA), were injected unilaterally into the temporal neocortex. FB and DY are dyes transported retrogradely, in contrast to FR and BDA which are transported bidirectionally, however, their anterograde transport was more intense than the retrograde one.

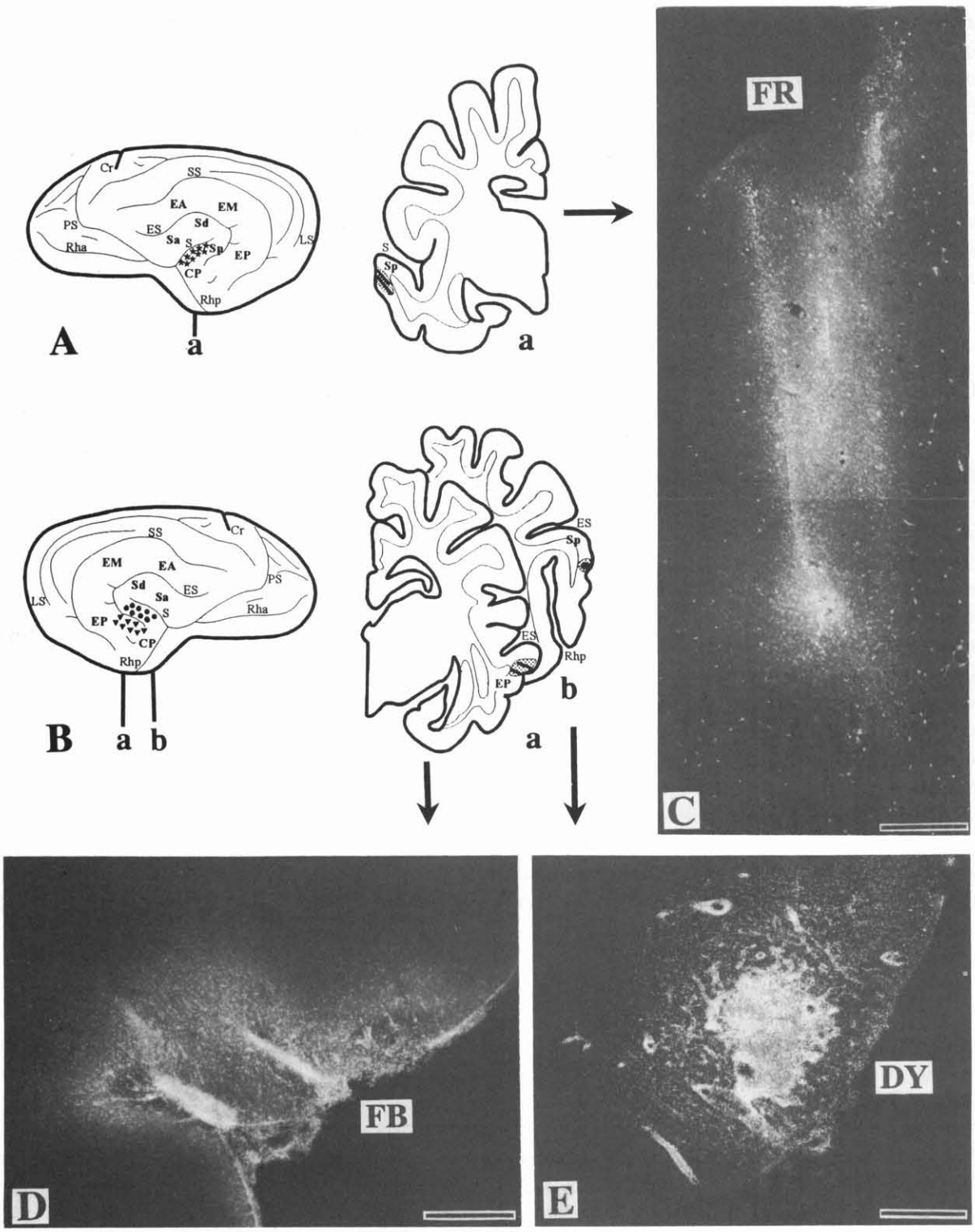

Fig. 1. Diagrams and low-power photomicrographs of coronal sections through the temporal neocortex illustrate examples of injections of three fluorochromes. A, localization of fluoro ruby (FR) injections (asterisks) in the posterior Sylvian gyrus (Sp) in D11,L is shown on the diagram of the left hemisphere and on the drawing of the coronal section from the marked level (a). B, localizations of fast blue (FB) (solid triangles) and diamidyne yellow (DY) (solid circles) injections in the posterior ectosylvian (EP) and posterior Sylvian areas respectively, in D6, are shown on the diagram of the right hemisphere and drawings of the coronal sections from the marked levels (a,b). C-E, photomicrographs of FR, FB and DY injections.

Injections were carried out under aseptic conditions. Animals were initially premedicated with Combelen (0.2 ml/kg) and 0.05% atropine (0.2 ml/kg) and then anesthetized with ketamine (Calypsol, 35 mg/kg). During surgery additional amounts of anesthetic (8.5 mg/kg) were given to maintain the proper level of anesthesia throughout the experiment. The selected areas of the temporal cortex were exposed by a craniotomy and cutting of overlying dura matter.

Multiple pressure injections were made through a glass micropipette adjusted to a picospritzer (General Valve Corporation). At a single cortical site approximately 50 nl of dye was injected. The total amount of injected dye varied (0.5-3.0 µl), depending on the number of points of injection in a particular cortical area.

Three to four weeks after surgery animals were deeply anesthetized and perfused intracardially with 0.9% saline mixed with heparin, followed by 4% formaldehyde in 0.1 M phosphate buffer (pH 7.4) and 5% glycerol in the same buffer.

The brains were processed according to the cryoprotection method for frozen sections (Rosene et al. 1986).

Coronal frozen sections, 50 µm thick, with 500 µm distance between particular sections, were collected in phosphate buffer. Six separate sets of adjacent histological sections were prepared. Three sets were used for the examination of cells and axons labeled with fluorescent dyes or BDA. Two sets were reacted for AChE activity according to the method of Geneser-Jensen and Blackstad (1971). The sixth set was dehydrated and stained according to the standard Nissl method. Sections examined with fluorescent microscopy were not counterstained. These sections were coverslipped with Fluoromount (Serva), omitting the dehydration process.

Using fluorescent microscopy, labeled neurons were identified by blue perikaryon fluorescence for FB, green-yellow for neuronal nuclei labeling by DY (violet filter of Nikon EX 380-425), red for perikaryon and axon labeling by FR (green filter of Nikon EX 510-560).

For anterograde and retrograde labeling with biotynylated dextran amine (BDA), a modified procedure of Veenman et al. (1992), Brandt and Apkarian (1992) and Kisvarday et al. (1993) was applied. In comparison to the above-mentioned procedure, the following changes were introduced: 1) inhibition of endogenous peroxidase, 2) low concentration of Triton X-100 (0.05%) during incubation with ABC Kit, and 3) intensification of reaction product with heavy metals according to the procedure of Adams (1981).

BDA (Molecular Probes) was dissolved in saline at a 10% concentration. After sectioning on a freezing microtome, free-floating sections were rinsed in 0.01 M phosphate buffered saline (PBS) and incubated for 5 min. with 10% methanol and 3% hydrogen peroxide in PBS to inhibit endogenous peroxidase activity (Totterdell et al. 1992). After rinsing the sections were preincubated in PBS containing 0.05% Triton X-100 (Sigma) and then incubated overnight with Vectastain ABC Standard Kit (Vector), 1:400 with 0.05% Triton X-100 in PBS. Subsequently the sections were thoroughly rinsed in PBS. The peroxidase component of the avidin-biotin complex was visualized according to nickel-cobalt DAB procedure as follows: the sections were preincubated in a mixture of 0.05% DAB (Sigma) in PBS, 1% cobalt chloride and 1% nickel ammonium sulfate and then hydrogen peroxide was added to a final concentration of 0.005% in which the sections were additionally incubated for 5-10 min. The sections were rinsed in solutions of heavy metals and then in PBS. Finally, sections were mounted on gelatin-coated slides, air-dried, cleared and coverslipped with DPX (Serva).

Locations of labeled cells and axon terminals were established according to the position of blood vessels charted onto drawings prepared from sections.

RESULTS

The temporal neocortex in the dog (Fig. 2) includes the anterior (EA), middle (EM) and posterior (EP) ectosylvian areas, the anterior (Sa), dorsal (Sd) and posterior (Sp) divisions of the Sylvian gyrus (except its most anteroventral region) as well as the anterior part of the posterior composite gyrus (CP). Dorsally and caudally, the temporal cortex is limited by the suprasylvian sulcus (SS), whereas ventrally, by the posterior rhinal sulcus (Rhp). Rostrally, the temporal cortex extends to the insular granular cortex of the anteroventral part of the Sylvian gyrus and the somatosensory cortex situated in the most anterior region of the ectosylvian gyrus. Kreiner's (1966) terminology was adopted in the description of subdivisions of the temporal neocortex. The parcellation of the temporal cortex was additionally verified by defining the dominant thalamo-cortical connections taking rise from the particular auditory nuclei of the medial geniculate body and the associative nuclei of posterior thalamus (Malinowska and Kosmal, in preparation).

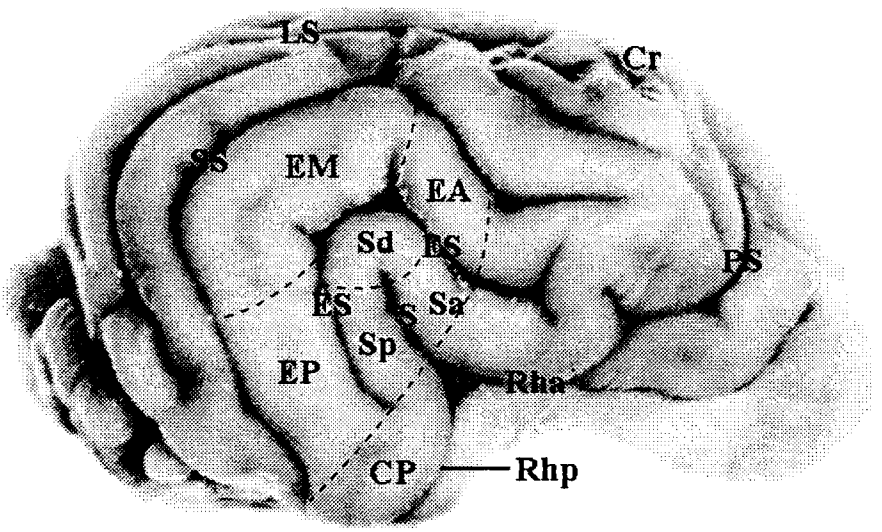

Fig. 2. Photograph of the lateral view of the right hemisphere of the canine brain. In the temporal cortex sulci and subdivisions of gyri are marked (see detailed description in the Results). Magnification 1.5 x.

Localization of injections

Injections of fluorescent dyes and BDA were made into the canine temporal neocortex, covering the ectosylvian and Sylvian gyri as well as the anterior area of the posterior composite gyrus (Fig. 3). Usually two or three fluorochromes, or fluorochromes and BDA, injections were placed in the same dog, in order to determine the precise topography of connections, particularly connections of the cortical fields surrounding the primary auditory cortex whose morphofunctional organization is not known. Localization of particular injections of all experimental cases is illustrated in Fig. 3.

The area EA was injected in two dogs: D1 (FR, DY) and D2 (DY). In D1, injection of DY was located in the anterior part of EA whereas FR injection was placed in the adjoining caudal part of EA. In D2, the DY injection was situated at the border of two areas, the caudal part of EA and anterior part of EM.

The area EM was injected in three dogs: D2 (FR), D3 (FB, DY, FR) and D5 (FR, DY). In D2, injection of FR was situated in the intermediate part of EM, whereas in D3, the injections of three fluorochromes were placed adjacent to each other covering the majority of area EM. Injections in D5 were placed in the rostral (DY) and caudal (FR) parts of area EM, close to the ectosylvian and suprasylvian sulci, respectively (ES, SS, Fig. 3).

The area EP was injected in seven dogs. Injections were placed successively from the dorsal to ventral direction. The majority of injections covered separately the rostral or caudal parts of the gyrus bordering the ectosylvian or suprasylvian sulci. One injection (D8, DY) was placed at the border of two adjacent areas, posteroventral EM and posterodorsal EP.

A selective injection into the dorsal EP zone was made in D4 (FB, DY, BDA). In this case FB and DY injections were placed caudally in the part of EP bordering the suprasylvian sulcus, whereas BDA injections were located in the rostral region of the gyrus, bordering the ectosylvian sulcus. In the rostral part of area EP, along the ectosylvian sulcus were located large FB injections in D5 involving both the dorsal and ventral zone of area EP.

The ventral EP zone was injected in four dogs: D6 (FB), D7 (FR), D10 (DY) and D11,R (DY and FB, right side). The FB injections in D6 were located similar to those in D5 in the rostral part of EP, however, in D6 it covered a more ventral extent of EP. The DY injections in D10 involved similar anteroventral EP region. The FR injection in D7 was situated across the ventral EP, between posterior ends of the ectosylvian and suprasylvian sulci, whereas a similarly situated DY injection in D11,R

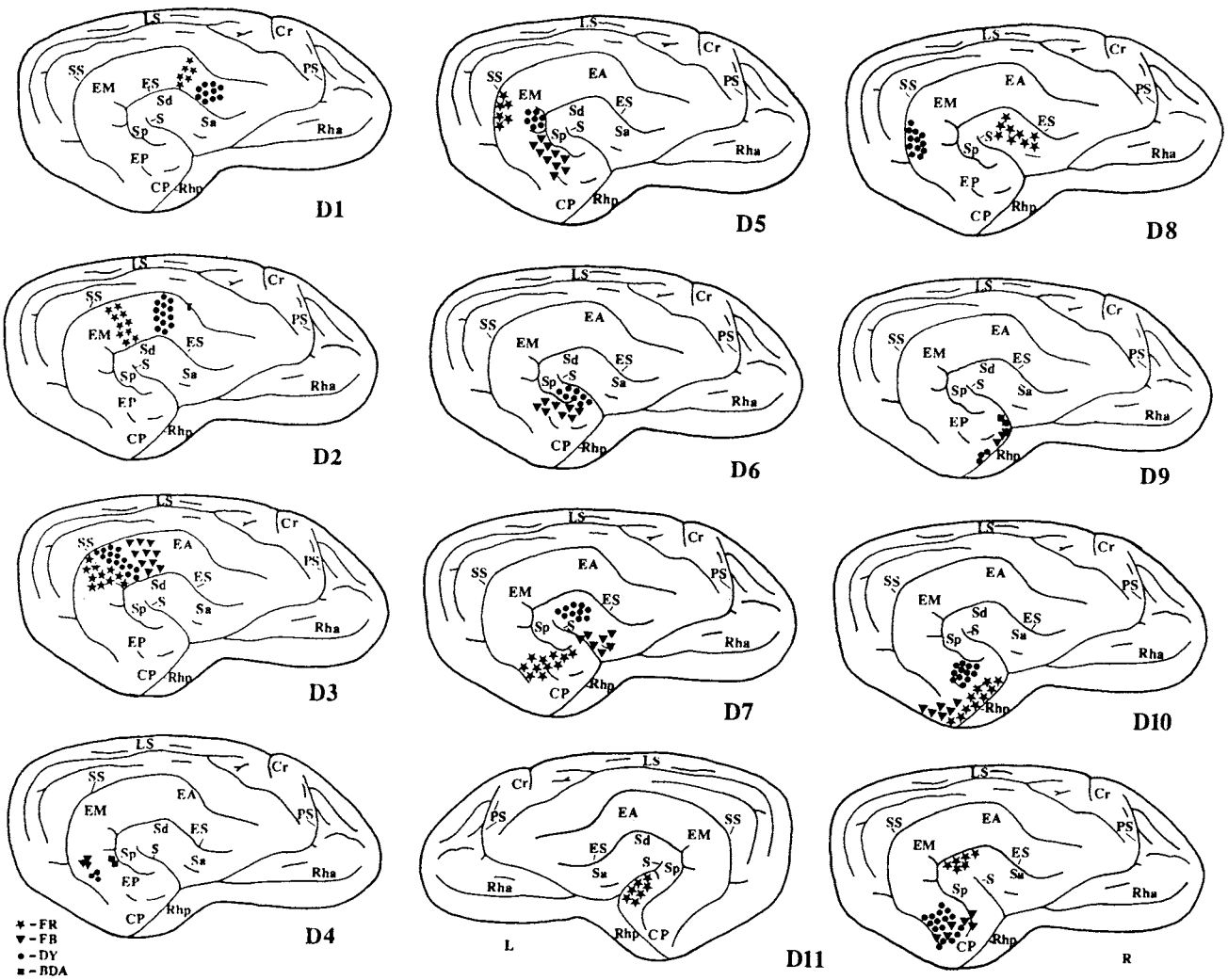

Fig. 3. Sites of injections in particular dogs used in the study. Injections are marked on diagrams of lateral view of hemispheres. Three symbols represent fluorochrome injections: FB, solid triangles; DY, solid circles; FR, asterisks. Site of biotynylated dextran amine (BDA) injection is marked with solid squares. Remaining symbols - in abbreviations.

partly overlapped with the FB injection in the most ventral extent of the ectosylvian gyrus.

The area CP was injected in two dogs: D9 (BDA, FB, DY) and D10 (FR, FB). Small BDA, FB and DY injections in D9 were placed close to each other, along the rostral border of area CP where BDA injection covered the most dorsal CP part, adjacent to the ventral Sp. The FR injection in D10 occupied an area in the anterior part of CP along the dorsal bank of the posterior rhinal sulcus (Rhp), whereas the FB injection was situated more caudally, below the ventral tip of the suprasylvian sulcus, involving additionally a small posterior part of the posterior composite gyrus.

The Sylvian gyrus was injected in four dogs: D6 (DY), D7 (DY, FB), D8 (FR), D11,R (FR in right side), and D11,L (FR in left side). The area Sa was injected in D7 (FB), above the area designated in the cat as insular granular cortex (Krettek and Price 1978). The FR injection in D8 was placed slightly more dorsally, at the border of anterior and dorsal areas of the Sylvian gyrus. The area Sd was separately covered by the DY injection in D7 and the FR injection in D11,R. The FR injection was placed in the ventral wall of the middle ectosylvian sulcus and a small area of gyrus convexity. The area Sp was injected in D6 and D11,L. Both injections, DY in D6 and FR in D11,L, were located in the similar Sp region, along the posterior wall of the Sylvian sulcus and above the posteroventral part of the ectosylvian sulcus.

Additional control injections were made in the surrounding cortex of the most anterior ectosylvian zone, as

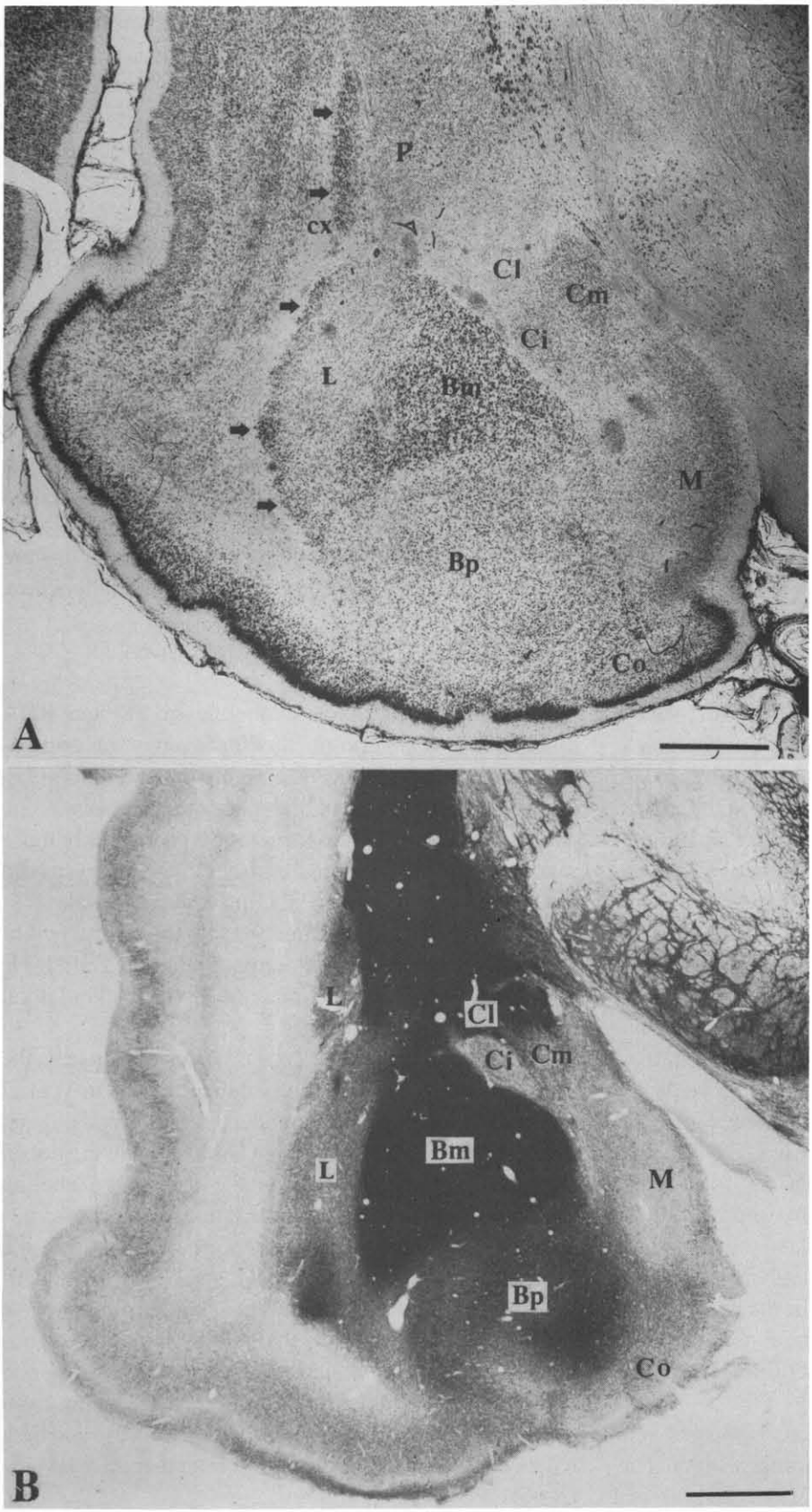

Fig. 4. Low-power photomicrographs of coronal sections through the intermediate level of the amygdala. A, Nissl stained section illustrates the cytoarchitecture of the dog amygdaloid complex. Note well visible, deeply stained, pericapsular population of neurons in the lateral nucleus, which are extended into the dorsal tip of the nucleus (arrows), situated between the external capsule fibers (cx) and the putamen (P). The central nucleus is divided into three subdivisions differing in size of neurons and intensity of staining. The medial subdivision (Cm) has larger neurons than remaining subdivisions. The intermediate (Ci) and lateral (Cl) subdivisions are less distinct in their cellular picture but clearly differentiated on the basis of AChE staining (see below). B, AChE stained section at the amygdaloid level comparable to that in A, illustrates a differentiation of AChE activity in amygdaloid nuclei. Note the highest AChE level of activity in Bm (most darkly stained) and different AChE activity in three parts of the central nucleus, low - in Ci, intermediate - in Cm and high - in Cl. The Cl shows only slightly lower AChE activity than dorsally adjacent putamen. Scale bars = 2.0 mm.

well as in the middle and ventral suprasylvian areas. There was no labeling in the amygdaloid nuclei after these control injections.

Distribution of labeling in the amygdala

AMYGDALOID NUCLEI CONNECTED WITH THE TEMPORAL CORTEX

The nomenclature and parcellation of the amygdaloid nuclei in the canine brain was previously described on the basis of differences in cytoarchitecture and the distribution of AChE activity (Kosmal and Nitecka 1977). The amygdaloid complex related to the temporal neocortex involved four nuclei: lateral, basal magnocellular, basal parvocellular, and lateral part of the central nucleus. The basal magnocellular and parvocellular nuclei in dog correspond, respectively, to the basal lateral and the basal medial nuclei of the cat and rat (Krettek and Price 1978).

The most distinctive cytoarchitectonic component of the amygdala is the basal magnocellular (Bm) nucleus due to the dominance of large neurons, deeply stained in Nissl method (Fig. 4A). Its borders are very sharp at the middle and posterior levels of the amygdaloid complex, whereas a population of large Bm neurons diminish in number rostrally and are intermixed with smaller neurons of the adjoining anterior area, which cause its anterior border to become somewhat less distinctive. The Bm nucleus, like in other species, is characterized by the darkest AChE staining indicating the highest level of AChE activity in the amygdala, uniform throughout its whole extent (Fig. 4B).

The vertically elongated lateral (L) amygdaloid nucleus is located laterally to the Bm. There is a narrow band of medium size, densely packed and more darkly stained neurons situated along its lateral border (Fig. 4A; arrows), adjoining the external capsule (cx) fibers. These pericapsular neurons continue dorsally and form a separate population which is visible above and laterally to the central amygdaloid nucleus, between the cx and the putamen (P). A large extent of the lateral nucleus shows a moderate level of AChE activity. In the anterior and posteroventral parts of the nucleus there are, however, small patches of higher AChE activity (dark patches in L; Fig. 4B).

The basal parvocellular (Bp) nucleus is located ventrally to Bm (Fig. 4A,B). Its ventral border with the cortical amygdaloid nucleus (Co; Fig. 4A,B) is less distinct than the dorsal one in both Nissl and AChE staining. In the medial extent of Bp a distinct group of larger neurons could be observed in comparison with that in the rest of the nucleus (at the more caudal level of the nucleus than that presented in Fig. 4A). They partially overlap with an area of higher AChE activity observed in the medial region of the nucleus (Fig. 4B).

The central nucleus (C) is situated above Bm and below the putamen (Fig. 4A,B). In the dog, the central nucleus is not homogeneous and on the basis of differences in size of neurons and level of AChE activity it can be divided into three subdivisions (Kosmal and Nitecka 1977), but only its lateral part receives an amygdalopetal projection. The border between the putamen and the lateral part of the central nucleus can be difficult to define due to similar cytoarchitecture and AChE activity in both structures. The lateral part of the central nucleus differs from dorsally adjacent putamen only by slightly lower AChE activity (Fig. 4B) and lack of large cells that are a characteristic feature of the putamen cytoarchitecture.

CORTICO-AMYGDALOID CONNECTIONS

The anterograde axonal labeling of FR and BDA allowed us to determine the topography of cortico-amygdaloid connections originating in the temporal neocortex, differentiated in both pattern and density.

Among injections into the temporal cortex only those involving the anterior area of the ectosylvian gyrus did not cause any anterograde labeling in the amygdala (EA; Fig. 3; D1), whereas FR injection into the central part of area EM revealed weak anterograde labeling of single axons reaching the dorsolateral part of the lateral amygdaloid nucleus (Fig. 5).

Injections in the area EP, placed successively from the dorsal to ventral direction, visualize the dorso-ventral gradient of increasing axonal density of amygdalopetal connections. BDA injections in D4 located in the dorsal EP zone (Fig. 6; see diagram on the top) caused labeling of sparse axons directed to the lateral amygdaloid nucleus. Their terminals were seen predominantly in the postero-lateral part of the nucleus (L; Fig. 6A and B; dotted sites), however, at the most caudal limit, sparse axons were scattered into the medial extent of the nucleus. They form short side branches with a few synaptic boutons (Fig. 6C; arrowheads). The axons arising from the dorsal part of EP were slightly more profuse and they reached more caudal regions of L than that after EM injection.

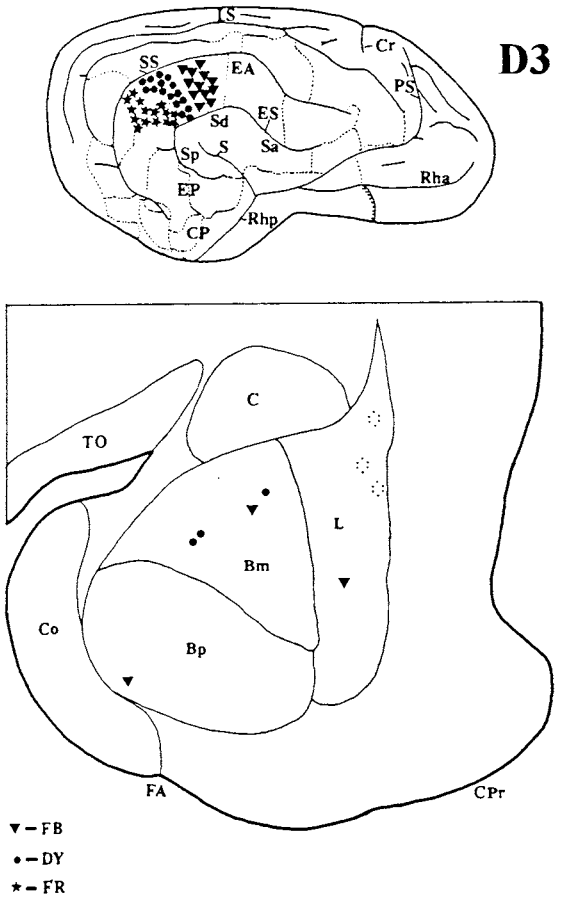

Fig. 5. Distribution of labeling in the amygdaloid nuclei after injections into the area EM, in D3. Localization of FB (solid triangles), DY (solid circles) and FR (asterisks) injections are marked on diagram of the right hemisphere on the top. On the diagram of coronal section of the amygdala (illustrated at the bottom) a distribution of FB, DY and FR retrogradely labeled cells (the same symbols as injections) and anterogradely labeled terminals (dots) is marked.

In the case of the FR injections into the ventral EP zone (D7; Fig. 7; see diagram on the top) plentiful axons penetrate a large antero-posterior extent of the lateral amygdaloid nucleus. Anteriorly, axons reach predominantly the dorsal tip of L (Fig. 7A,B). In successive caudal sections, they extended more ventrally, covering the lateral (Fig. 7C-F) and intermediate (Fig. 7D,E) regions of the nucleus. The terminal plexus of very thin axons was distinctly more dense along the pericapsular extension of the nucleus, in comparison to the middle nucleus region, whereas its most medial part remained free of labeling (Fig. 7C-E). A striking difference in density of corticofugal axons after dorsal and ventral EP injections indicates that this projection significantly increases along the ectosylvian gyrus.

In the case of D7, in addition to labeling in the lateral nucleus, axonal terminals were also found in the small postero-lateral region of the central nucleus (C; Fig. 7D-F).

Injections into the area CP resulted in labeling of axons directed into four amygdaloid nuclei: lateral, central, basal parvocellular, and basal magnocellular. The most dense labeling was observed in L (D10; Fig. 8A-F). Even though the distribution of labeling was similar to that after EP injections it appeared to be wider. In D10, where FR injections covered a large part of area CP, axonal terminals were distributed through the entire rostrocaudal extent of the nucleus. In the lateral sector of the nucleus, thin axonal terminals were extremely dense as compared with those distributed medially, and extended from the anterodorsal tip to the most posterior limit of the nucleus (L; Fig. 8A-F). Less dense terminals occupied the medial sector of the nucleus while leaving its most medial part free of labeling (Fig. 8A,B,D,E) as in cases of the ventral EP injections (cf. Figs. 7 and 8). A small BDA injection in D9 was placed in the most dorsal CP part, at the border with the posterior Sylvian gyrus (Fig. 9; see diagram on the top). In this case, axonal terminals were also very dense in the lateral amygdaloid nucleus, although the extent of labeling was more limited in comparison with that in D10. Axonal terminals were accumulated in separate groups along the anterior and intermediate level of the lateral nucleus. The largest accumulation of thin axons with numerous terminal boutons was found in the most anterodorsal, pericapsular tip (Figs. 9A,B and 10A) and ventrally in the lateral part of the nucleus (Figs. 9A-C; densely shaded areas and 10B). The area of this intense labeling occupies slightly more medial part of the nucleus at the intermediate level of amygdala, in comparison to that in D10. Additionally, a less dense axonal plexus was seen around the dense terminals (Fig. 9A-F; sparsely dotted area). Sparse, parallel axons with varicosities and numerous boutons located along them were seen in the most ventral extent of L (Fig. 10C; double arrowhead and single arrowheads, respectively).

Injections into CP resulted in the labeling of amygdalopetal axons in C, Bp and Bm amygdaloid nuclei. BDA injection in D9 and FR in D10 revealed the labeling of axons distributed in the lateral part of C (Figs. 8C-E and 9A-D) and clearly differentiated in thickness, with occasional varicosities (Fig. 11A; double arrowhead) and only a few terminal boutons (Fig. 11A; arrowheads). In

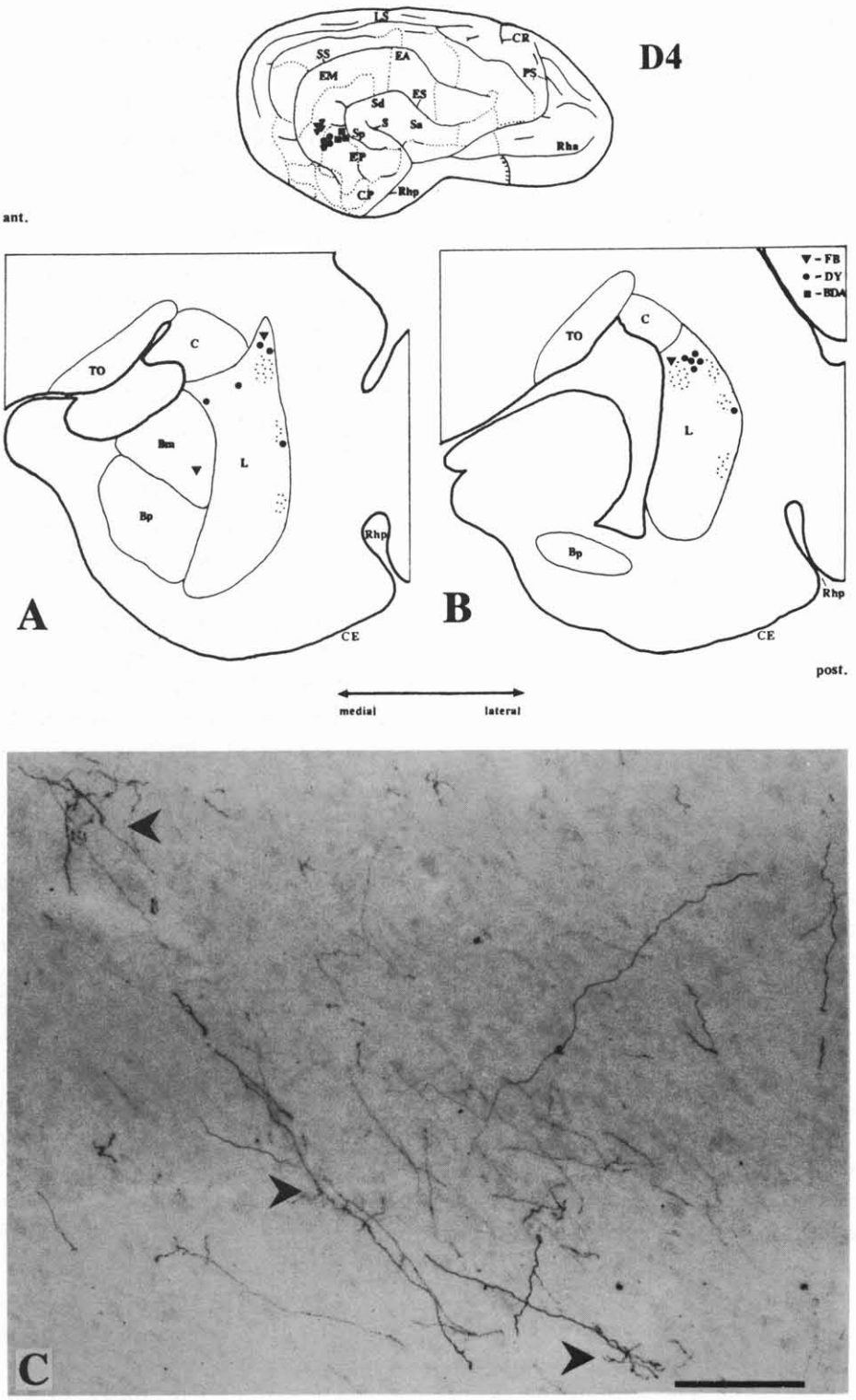

Fig. 6. Distribution of labeling in the amygdaloid nuclei after injections into the dorsal zone of the area EP, in D4. Localization of FB (solid triangles); DY (solid circles) and BDA (solid squares) injections are marked on diagram of the right hemisphere on the top. A,B, distribution of retrogradely FB and DY labeled cells in the amygdaloid nuclei, marked with the same symbols as injections, on the drawings of two coronal sections through the posterior amygdaloid level. Dotted sites indicate the localizations of BDA labeled axonal terminals in the lateral amygdaloid nucleus (L). C, photomicrograph of BDA labeled axons in the posterior region of the L. Sparsely distributed axons form short side collaterals, with single terminal boutons (arrows).

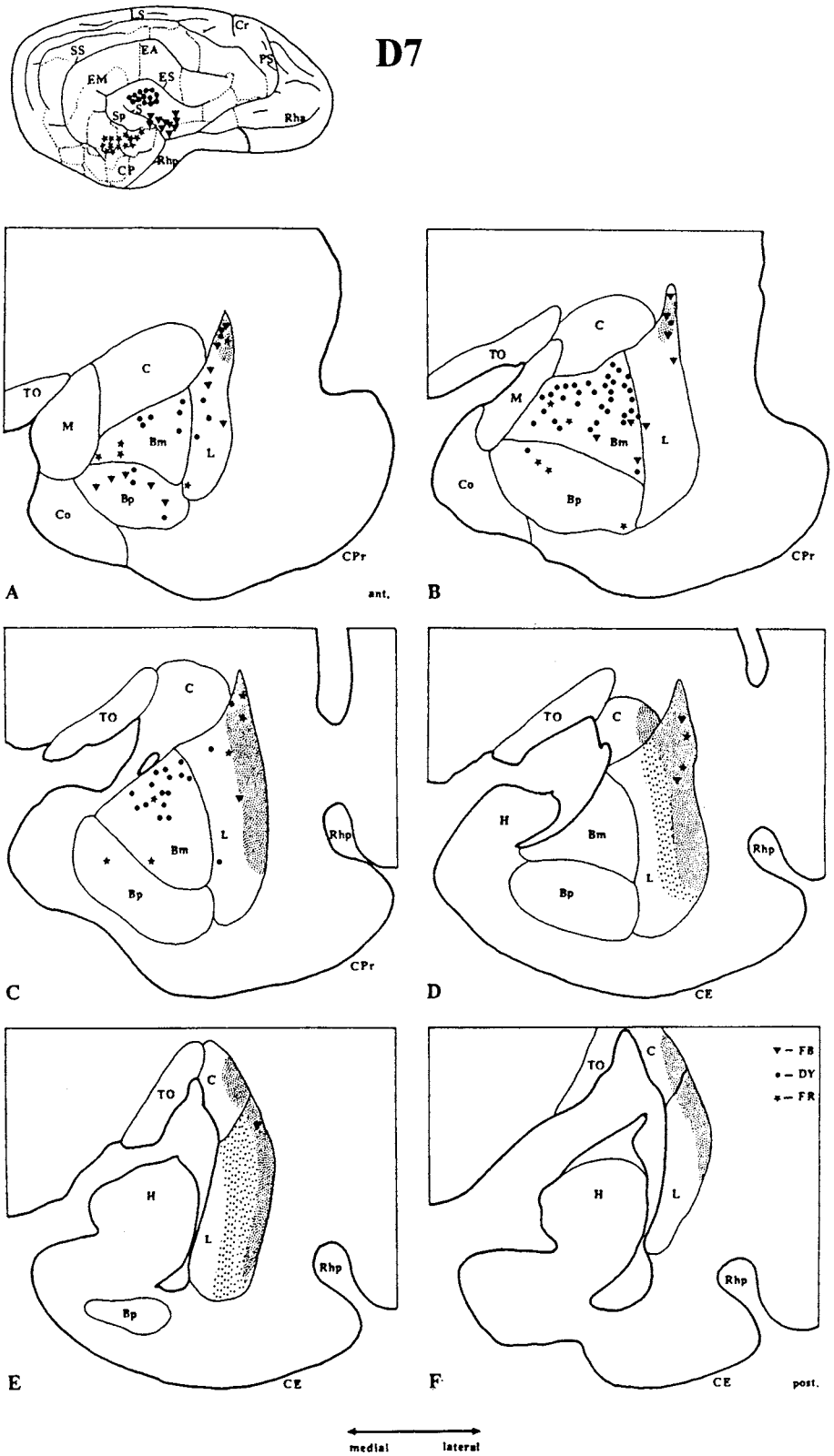

Fig. 7. Distribution of labeling in the amygdaloid nuclei, in D7. Localizations of fluorochrome injections in the Sa (FB - solid triangles), in the Sd (DY - solid circles) and in the ventral zone of the area EP (FR - asterisks) are shown on the diagram of the right hemisphere (on the top). Distribution of FB, DY and FR retrogradely labeled cells (the same symbols as injections) and anterogradely FR labeled axonal terminals, dense - shaded and sparse - dotted, are marked on six representative diagrams of coronal sections, from the anterior (A) to posterior (F) level of the amygdala.

this case, labeling in C was less intense in comparison with cases of injections located more ventrally in the area CP (cf. Fig. 9A-D with Fig. 8C-E).

In both cases of CP injections, labeled axons reaching the basal amygdaloid nuclei were sparse and extremely thin. BDA method in D9 visualized poorly arborized

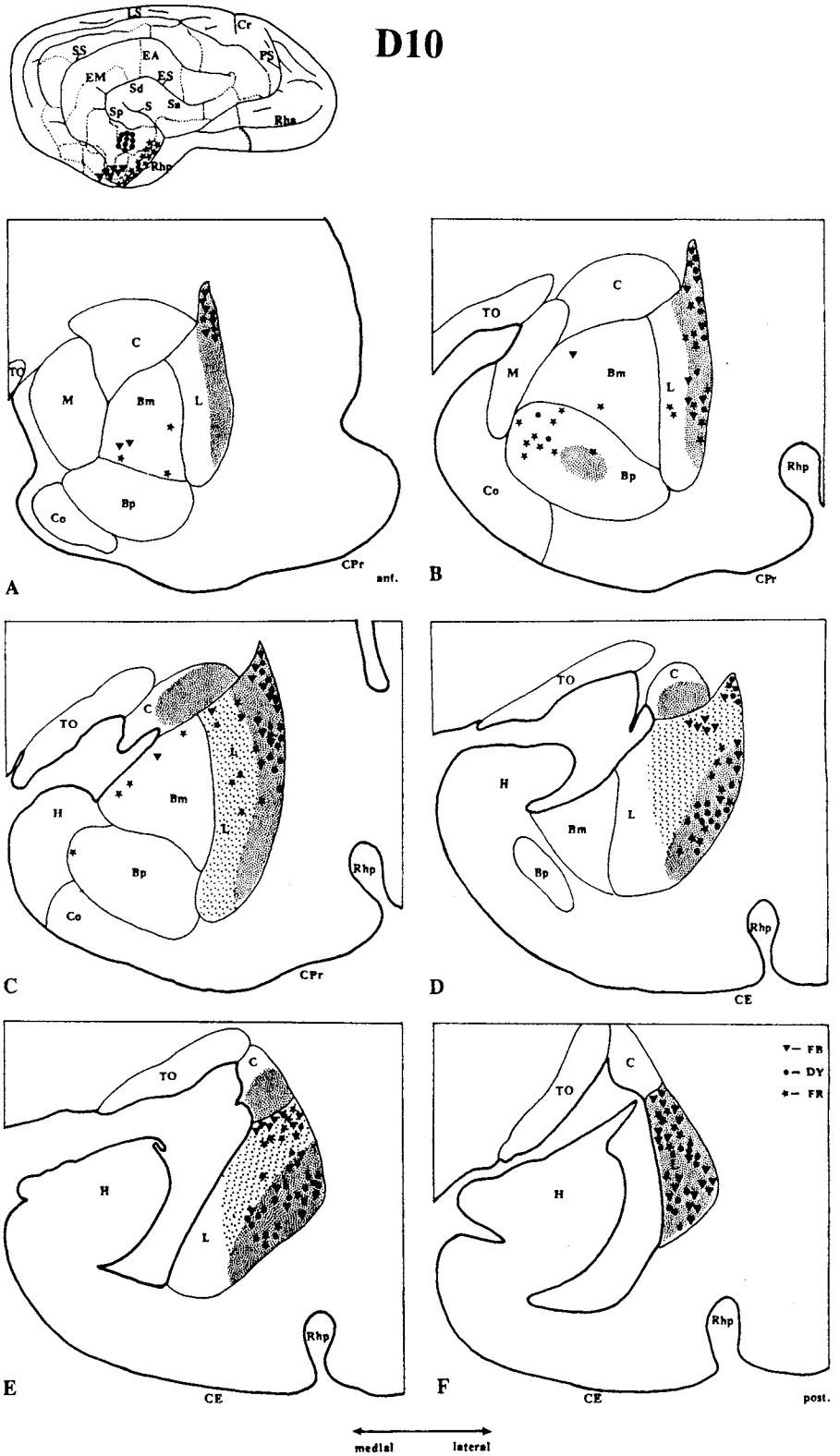

Fig. 8. Distribution of labeling in the amygdaloid nuclei, in D10. Localizations of fluorochrome injections in the ventral zone of area EP (DY, solid circles), in the anterior CP (FR, asterisks) and in the posterior CP (FB, solid triangles) are shown on the diagram of the right hemisphere (on the top). Distribution of FB, DY and FR retrogradely labeled cells (the same symbols as injections) and anterogradely FR labeled terminals, dense - shaded and sparse - dotted, are marked on six representative diagrams of coronal sections, from the anterior (A) to posterior (F) level of the amygdala.

axons with a few synaptic boutons reaching the central part of Bp nucleus (Figs. 9A-D and 11C). Moreover, only in this case, a few scattered axons in the dorsal part of Bm were found. Like in Bp they were extremely thin, but their terminal boutons seemed to be more numerous (Fig. 11B).

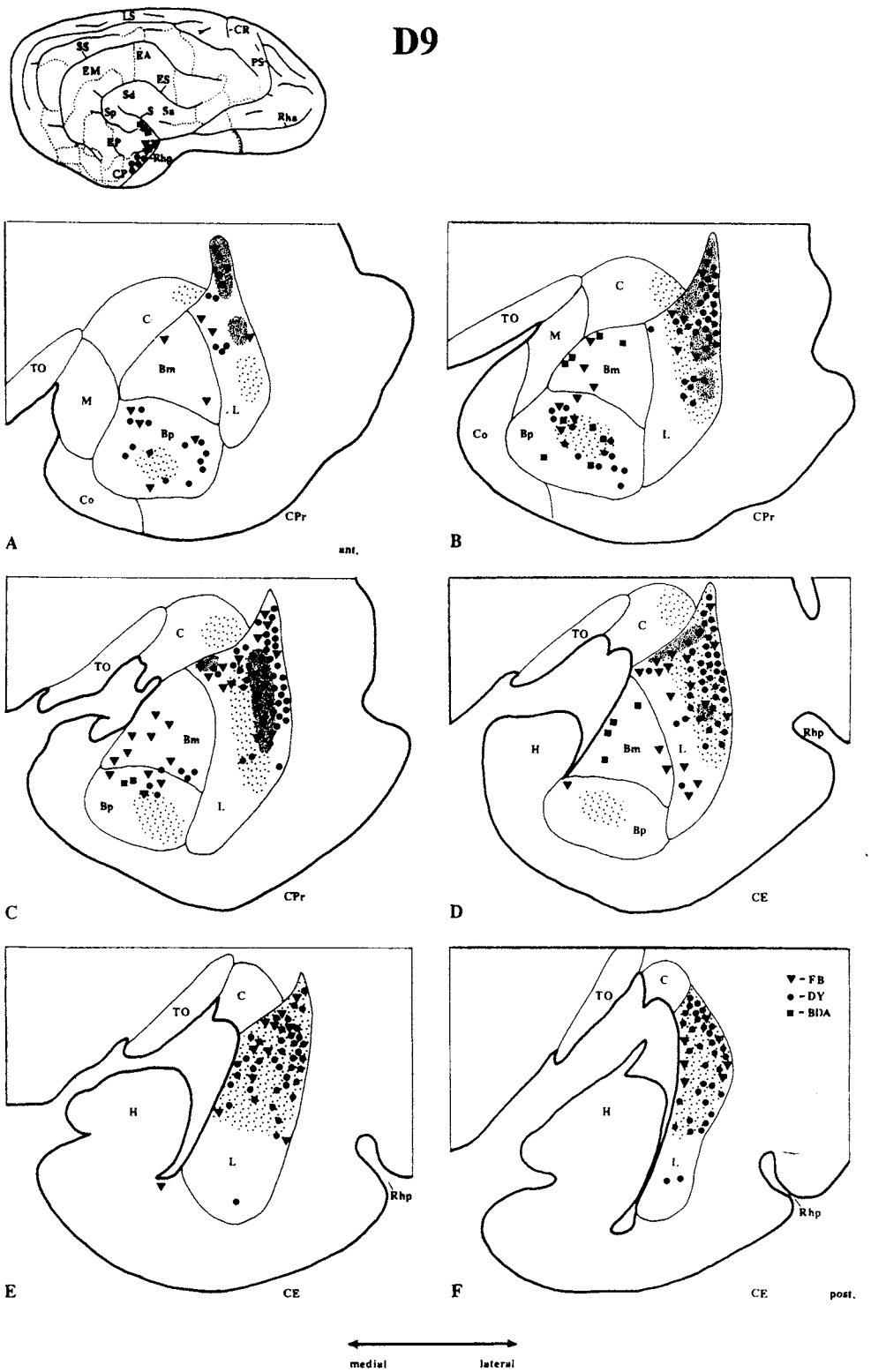

Fig. 9. Distribution of labeling in the amygdaloid nuclei after injections into the anterior part of area CP, in D9. Localizations of three injections: BDA (solid squares), FB (solid triangles) and DY (solid circles) are shown on the diagram of the right hemisphere (on the top). Distribution of FB, DY and BDA retrogradely labeled cells (the same symbols as injections), and anterogradely BDA labeled axonal terminals, dense - shaded and sparse - dotted, are marked on six representative diagrams of coronal sections, from the anterior (A) to posterior (F) level of the amygdala. Single BDA labeled cells are not marked on the diagrams. Their distribution is shown in Fig. 10A,B.

Injections of fluorochromes into the anterior, dorsal and posterior areas of the Sylvian gyrus showed that its three parts have specific connectional features.

The posterior Sylvian area constitutes an extension of the cortex sending intensive connections to the amygdala. The FR injection in D11,L (Sp; Fig. 12; see left diag-

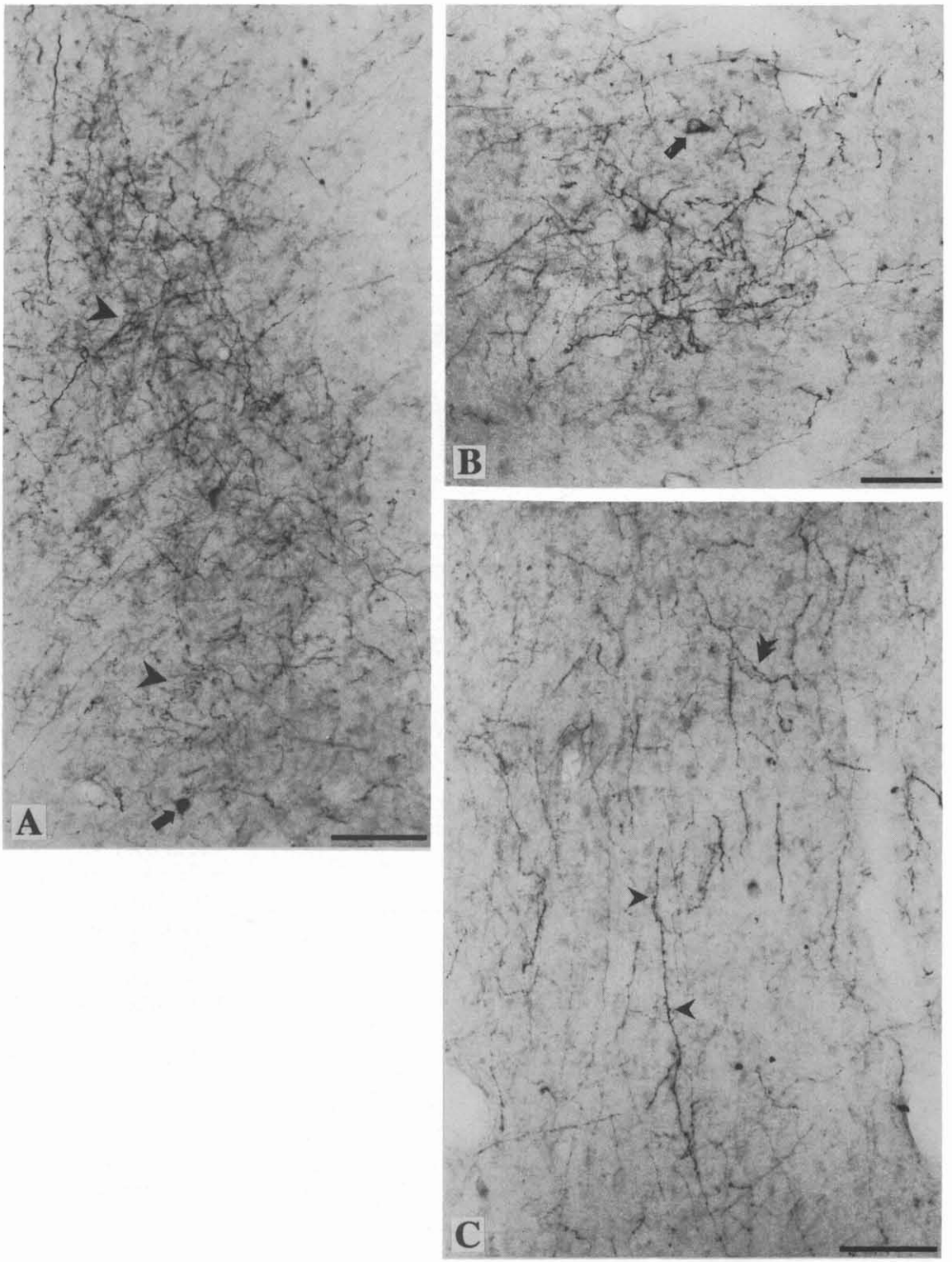

Fig. 10. High-power, photomicrographs of BDA anterograde labeling of axons in the lateral nucleus of D9, at the level of amygdala corresponding to Fig. 9B. A, dense axonal plexus, with numerous synaptic boutons (arrowheads), and single retrogradely labeled cells (arrow), seen in the most dorsolateral part of L. B, moderate in number, anterogradely labeled terminal axons and single retrogradely labeled cells (arrow) localized more ventrally than that in A, in the pericapsular part of L. C, a sparse, parallel arranged axons distributed in the ventral part of L, with varicosities (double arrowhead) and fairly numerous terminal boutons located along the axons (arrowhead). Scale bars = 0.1 mm.

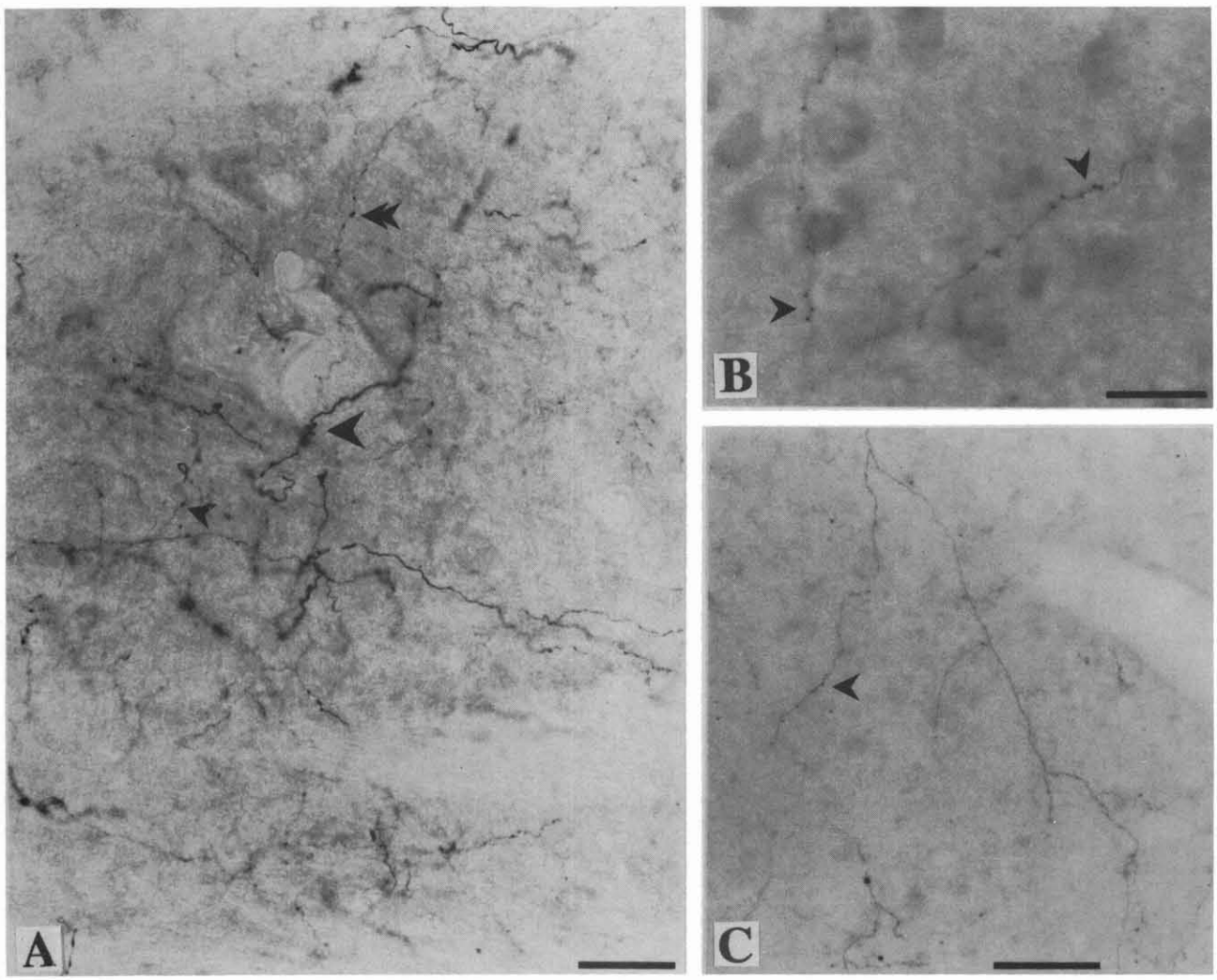

Fig. 11. High-power photomicrograph of BDA labeling in the amygdaloid nuclei of D9, at the level of amygdala corresponding to Fig. 9C. A, sparse, differentiated in thickness labeled axons in the posterolateral part of the central nucleus. Occasional varicosities (double arrowhead) and a few terminal boutons only (single arrowheads) are seen on the axons. Scale bar = 0.05 mm. B, thin axons with terminal boutons (arrowheads) penetrate occasionally the dorsal part of the Bm nucleus. Scale bar = 0.02 mm. C, an example of poorly arborized, thin axons, with single terminal boutons (arrowhead) observed in the central part of the Bp nucleus. Scale bar = 0.1 mm.

ram on the top) shows that amygdalopetal connections are formed by thin, moderately dense axons terminating in the small pericapsular part of the dorsolateral L tip (Fig. 12B,C - left) and the large extent of the intermediate part of the nucleus (Fig. 12A-C - left). The latter labeling seems to be the characteristic site of termination of a projection arising from the posterior Sylvian area. This distribution of terminals reflects the latero-medial topography within the L nucleus, when injections shift from area CP to area Sp (cf. Figs. 8, 9 and 12).

Sparsely distributed labeled axons also reach the ventrolateral part of C at the border with the L nucleus (Fig. 12A,C - left). Additionally, a single cluster of terminals was found slightly more dorsally in C (Fig. 12A - left). The amygdalopetal projection from the Sylvian gyrus reaching the central nucleus clearly decreases in density in comparison to that from area CP (cf. Figs. 8C-E and 12A,C).

In contrast to Sp, injection into the dorsal Sylvian area in D8 and D11,R resulted in labeling of sparse axonal terminals scattered in the dorsal (Fig. 12A - right; dotted areas) and intermediate L extent (Fig. 14B). The density of the projection from Sd seems to be comparable with that derived from the dorsal EP cortex, however, axons

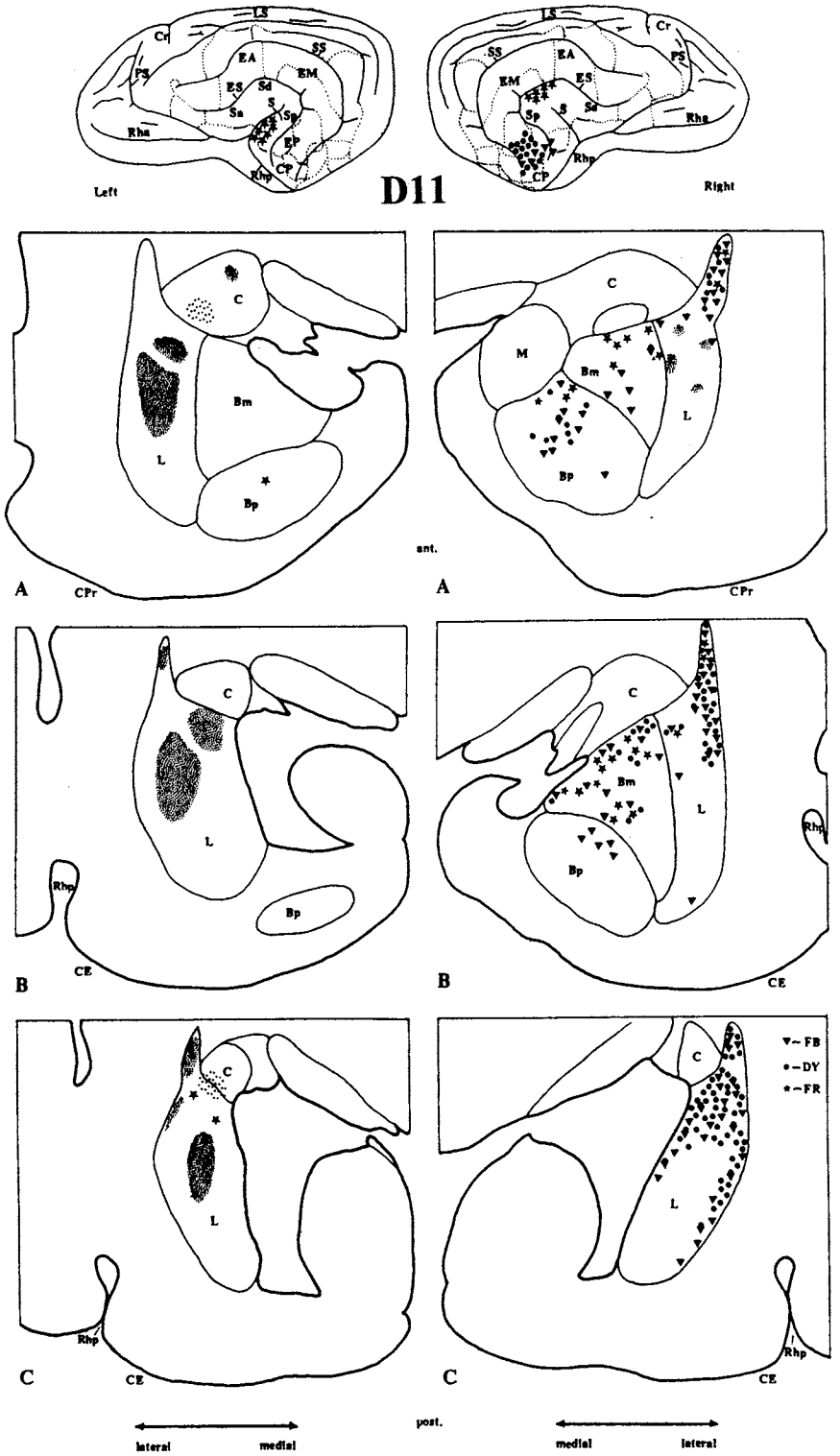

Fig. 12. Distribution of labeling in the amygdaloid nuclei, in D11. Left column: localization of FR injection in the Sp (asterisks) is shown on the diagram of the left hemisphere (on the top). Distribution of anterogradely FR labeled axonal terminals, dense - shaded and sparse - dotted, as well as single retrogradely labeled cells (asterisks) in the amygdaloid nuclei are shown in three representative diagrams of coronal sections, from the anterior (A) to posterior (C) level of the amygdala. Right column: localizations of fluorochrome injections in the Sd (FR, asterisks), and in the ventral zone of EP (DY, solid circles; FB, solid triangles) are shown on the diagram of the right hemisphere (on the top). Distribution of FB, DY and FR retrogradely labeled cells (the same symbols as injections) and anterogradely FR labeled axonal terminals (dots) are marked on three representative diagrams of coronal sections, from the anterior (A) to posterior (C) level of the amygdala. Note the single sites of axonal terminals and double-labeled cells (overlapped symbols of solid circles and triangles) in the dorsal L.

originating in the area Sd reach the more anterior part of L (cf. Figs. 6A,B and 12A - right).

The above observations show that along the ectosylvian and Sylvian gyri an intensification of the cortico-amygdaloid projection takes place. The dorsal part of the area EP sends only light projections that become more intense in the posteroventral extension. Thus, the area of origin of the most substantial amygdalopetal projections

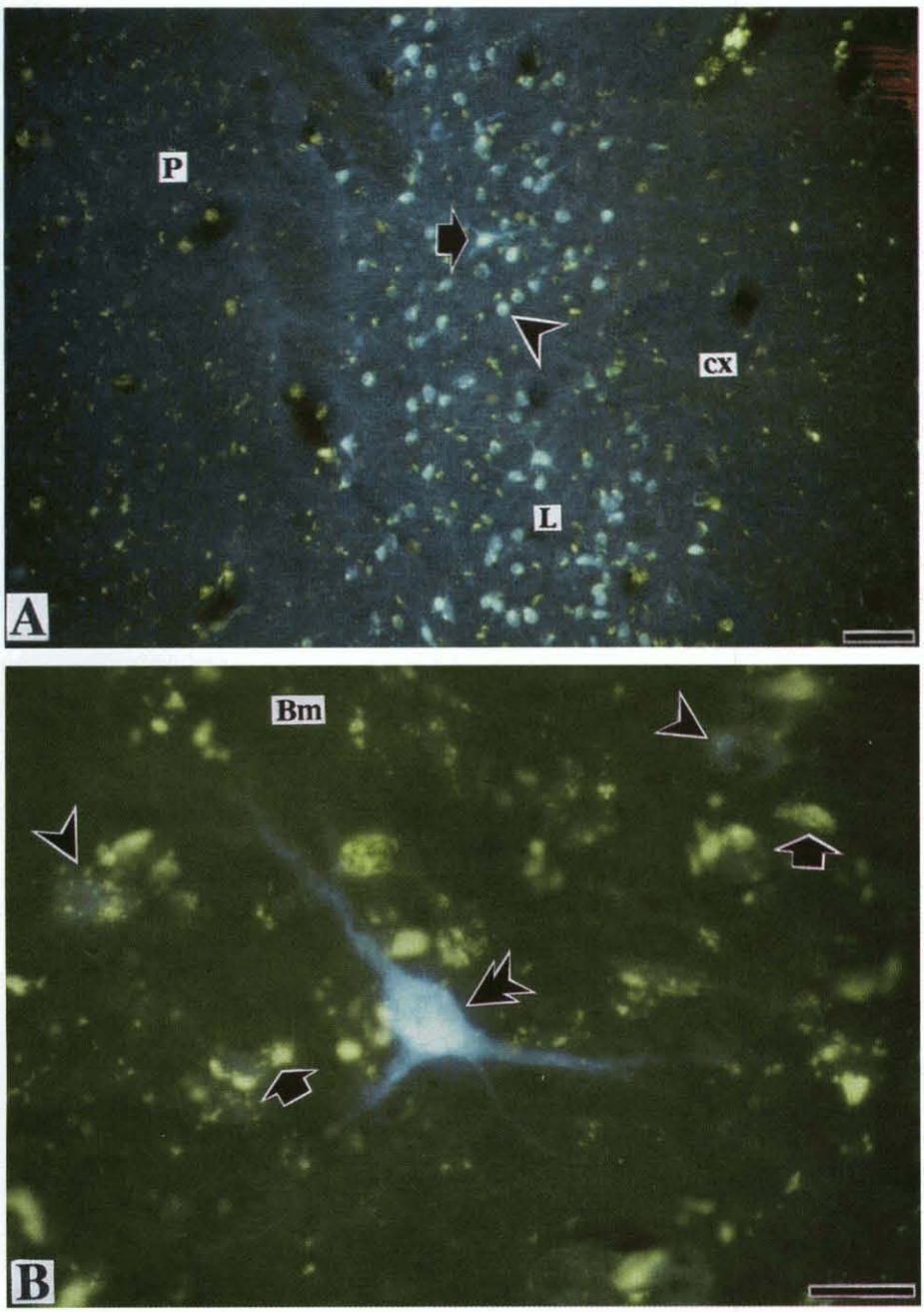

Fig. 13. High-power fluorescence photomicrograph of retrogradely labeled cells in the amygdaloid nuclei after injection into the ventral zone of area EP, in D11,R. A, retrograde labeling in the lateral nucleus, at the level corresponding to that in Fig. 12A (right column). FB neurons (arrow) and DY neuron nuclei (arrowhead) form cluster of cells within the most dorsal tip of the lateral nucleus situated between the putamen (P) and the external capsule fibers (cx). Scale bar = 0.1 mm. B, large FB labeled neuron in Bm nucleus (double arrowhead) situated at the level of amygdala corresponding to that in Fig. 12B. Inside the cell and in the background of the photomicrograph a yellow autofluorescence of a neuronal lipofuscin is seen (arrows). A few weakly FB labeled cells are marked with arrowheads. Scale bar = 0.03 mm.

involved the ventral extent of area EP, CP and Sp of the temporal neocortex. This projection disappears once again in the dorsal part of the Sylvian gyrus. Connections from areas EP and CP are predominantly directed into the lateral amygdaloid nucleus. In the nucleus latero-medial topography of corticofugal projection can be visualized by different localization of dense axonal terminals. Axons originating in the ventral part of the ectosylvian gyrus and in the posterior composite area are focused in the lateral, pericapsular sector of L, whereas in the medial L sector they are distributed more sparsely. The posterior Sylvian gyrus was defined as a source of a substantial projection terminating in the intermediate part of L.

Less profuse connections originating in the EP, CP and Sp neocortical areas are directed into the C, Bp and Bm amygdaloid nuclei.

AMYGDALO-CORTICAL CONNECTIONS

The topography of the amygdalo-cortical connections was determined on the basis of the distribution of

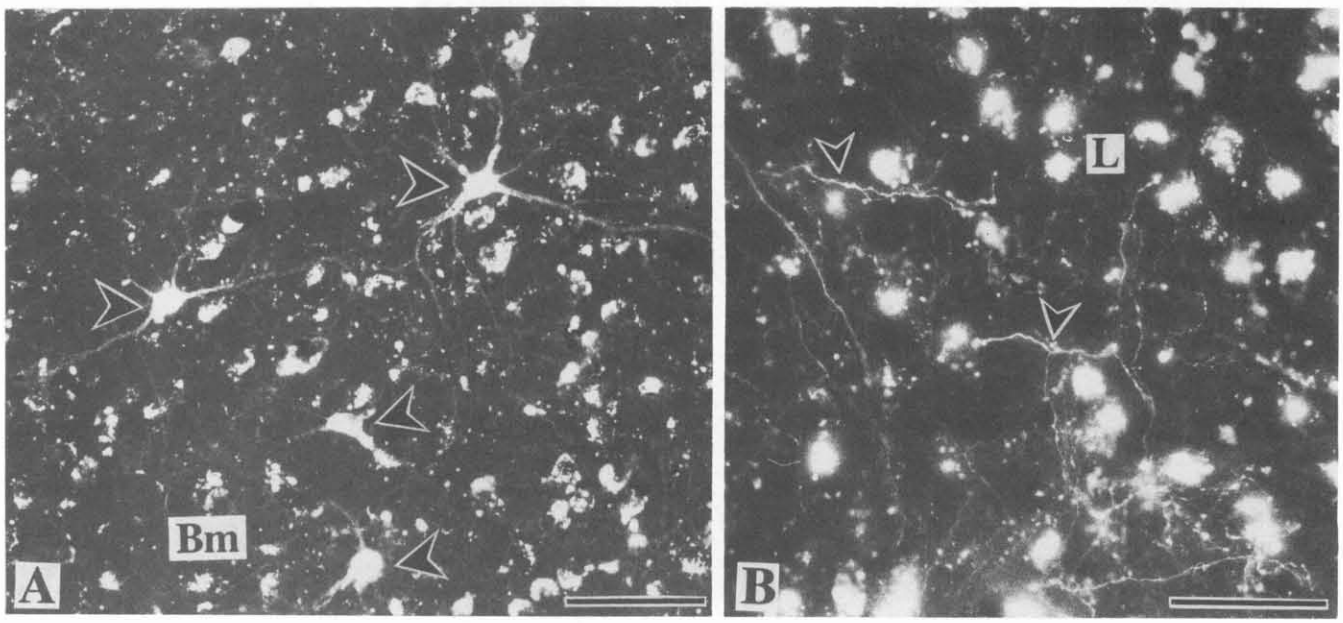

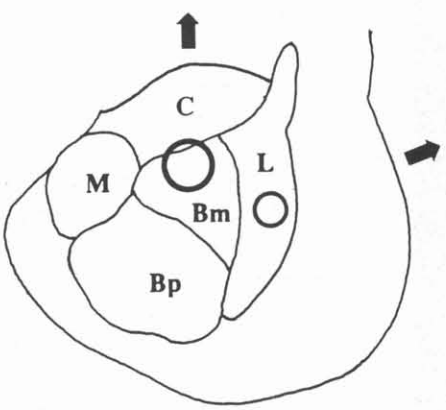

Fig. 14. High-power fluorescence photomicrograph of labeling in the amygdaloid nuclei following FR injection into the Sd, in D11,R. A, FR retrograde labeled cells in Bm nucleus (arrowheads), localized in the dorsal part of the nucleus (large circle on the scheme) at the border with the central nucleus (C), of the amygdaloid level corresponding to that in Fig. 12A (right column). B, sparsely distributed, retrogradely FR labeled axons (arrowheads) localized in the intermediate part of the lateral nucleus (small circle in enclosed scheme), observed at the amygdaloid level corresponding to that in Fig. 12A (right column). Scale bar = 0.05 mm. Note autofluorescence of numerous deposits of neuronal lipofuscin in the background of A and B. Scale bar = 0.1 mm.

amygdaloid neurons labeled retrogradely by FB, DY and FR injections into the temporal neocortex. Exceptions to this were injections into the EA (Fig. 3; D1, D2) which do not produce any retrograde labeling in the amygdaloid nuclei.

EM injections caused retrograde labeling of only single cells in the basal magnocellular and parvocellular nuclei as well as in the lateral nucleus. A majority of cells were localized in Bm nuclei (Fig. 5).

Following EP injections, retrogradely labeled cells were found in L, Bm, and Bp nuclei. In all cases labeled cells in the basal nuclei were scarce, whereas in L the retrograde labeling increased in number when injections were placed in the ventral EP zone in comparison to that following injection in the dorsal EP zone.

In the case of injections into the dorsal EP zone in D4 (FB and DY), single retrogradely labeled cells were found in the posterodorsal part of L and in Bm (Fig. 6A,B).

Following injections located in the ventral EP zone, labeled cells were found in L, Bm and Bp amygdaloid nuclei. As illustrated in D7 (Fig. 7A-C; asterisk), D10 (Fig. 8B-F; solid circles) and D11 (Fig. 12A-C; right, solid circles and triangles), labeled cells were accumulated predominantly in the pericapsular and posterior extent of L. In D11,R, as in previous cases, the most distinctive feature of retrograde labeling was an accumulation of cells in the dorsal pericapsular L sector (Figs. 12A,B - right; solid circles and triangles, and 13A) and in the posterodorsal part of this nucleus (Fig. 12C - right; solid circles and triangles). However, in this case only moderately numerous retrogradely labeled cells (FB, DY) were found in both basal nuclei (Figs. 12A,B and 13B). In comparison to labeling in D7 and D10, labeled cells were more numerous, probably due to the larger injection in D11. Mixed FB and DY injections in this case additionally caused many of the double-labeled cells to

appear in L (Fig. 12A-C; overlapped symbols of solid circles and triangles). In the remaining cases double--labeled cells in the amygdaloid nuclei were rather rarely observed.

The pattern of retrograde labeling following CP injections was very consistent with all markers. Retrogradely labeled cells were observed in the same amygdaloid nuclei as above, and the highest concentration of labeled cells was also seen in the L nucleus. In D9 and D10 (Figs. 8 and 9), the most numerous labeled cells were distributed along the lateral pericapsular sector of this nucleus (Figs. 8A-D; asterisks, solid triangles and 9A-D; three symbols). In the posterior amygdala, less dense retrograde labeling extended into the medial part of the L nucleus (Figs. 8C-E and 9C-D). Labeled cells increased in number at the most posterior L limit, where they were scattered throughout the almost entire area of the nucleus (Figs. 8E,F and 9E,F). However, in D9, where the injections were placed more dorsally in CP in comparison to D10, numerous labeled cells were distributed predominantly in the dorsal part of the nucleus, whereas the posteroventral part of the nucleus was free of labeling, (Fig. 9E,F).

Labeled cells in Bm and Bp were less numerous and located more anteriorly in comparison with those in L. (Figs. 8A-C; asterisks, triangles and 9A-D; three symbols).

The results of ventral EP and CP injections are very similar and demonstrate that both areas receive dominant connections originating in the cell population situated predominantly in the pericapsular region of the lateral nucleus and in its caudal extent. Projections from the

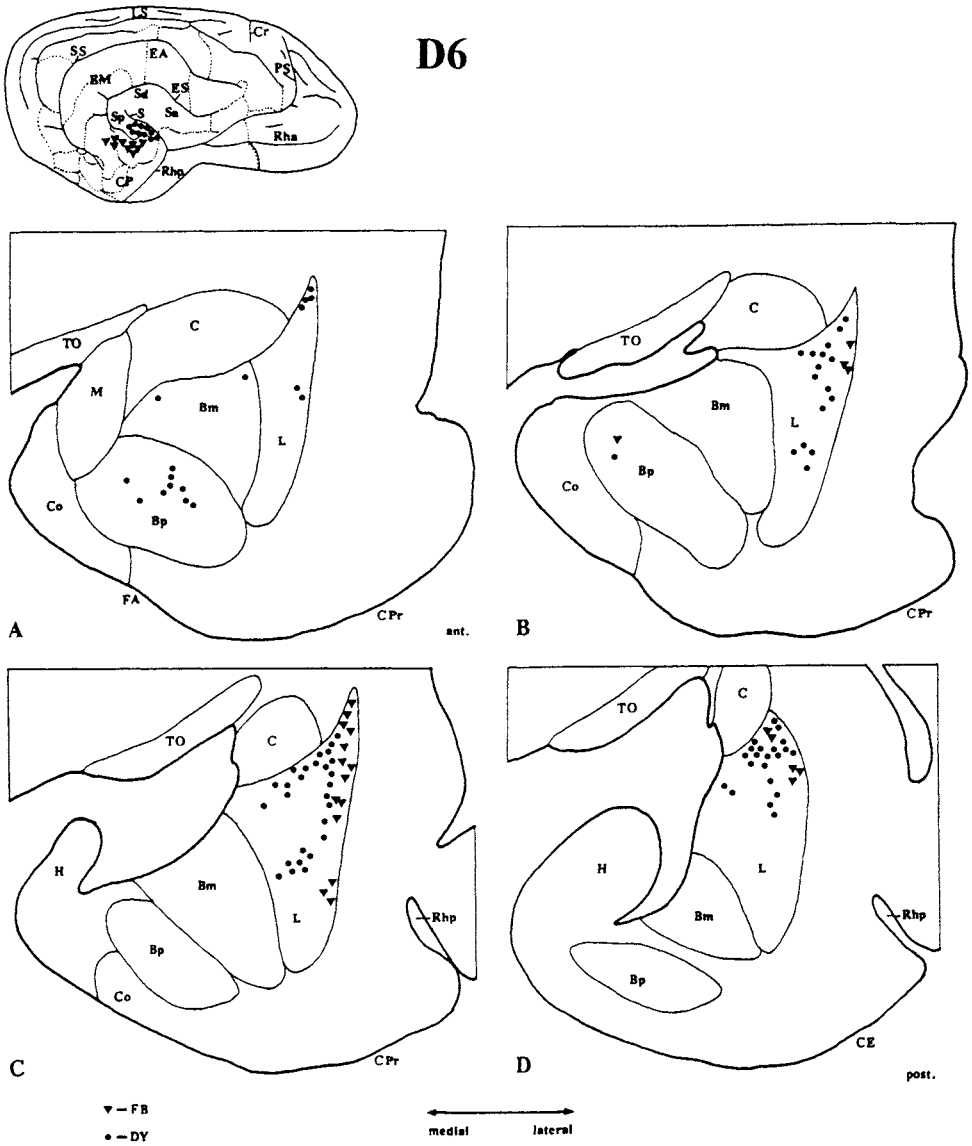

Fig. 15. Distribution of retrogradely labeled cells in the amygdaloid nuclei in D6. Localization of DY injection in the Sp (solid circles) and FB injection in the anteroventral EP extent (solid triangles) are shown on the diagram of right hemisphere (on the top). Distribution of FB and DY labeled cells (the same symbols as injections) is shown in four representative diagrams of coronal sections, from anterior (A) to posterior (D) level of the amygdala. Note that neurons of origin of projection to the area EP are located in the pericapsular L sector only, whereas neurons projecting to Sp are distributed through the intermediate nucleus region.

basal nuclei are less prominent. Fairly numerous cells giving rise to the projection were found only in the anterior half of both basal nuclei. The topography of the projections is marked by gradually increasing numbers of labeled cells from the anterior-dorsolateral to the posterior limit of the lateral amygdaloid nucleus, when injections were placed consecutively from the dorsal EP to cortex situated ventraly in areas EP and CP. This most substantial amygdalofugal projection is clearly focused in the most ventral part of EP and area CP.

Injections into the posterior, dorsal, and anterior Sylvian areas revealed significant differences in distribution of labeled cells supporting a division of the Sylvian gyrus into three parts.

Following injections into the posterior Sylvian area labeling was found in the lateral and basal nuclei. In D6 numerous labeled cells were observed mainly in the intermediate part of L nucleus (Fig. 15B-D; solid circles), whereas in the basal nuclei only a few labeled cells appeared in Bm and a slightly greater number of cells was found in the central part of Bp (Fig. 15A).

Comparing the results of DY and FB injections in D6 located in front and behind the ectosylvian sulcus in areas Sp and EP, respectively, it could be observed that the labeled cells form rather separated groups. The cells forming connections to the area EP are located at the most lateral, pericapsular limit of the nucleus (Fig. 15B-D; solid triangles), whereas the cells giving rise to a projection into the Sp are scattered more medially in the nucleus (Fig. 15B-D; solid circles). It is interesting to compare the density of labeling after two similarly placed injections into the posterior Sylvian gyrus: DY injection in D6 (Fig. 15) with FR injection in D11,L (Fig. 12; left). The latter injection resulted in retrograde labeling of only a few cells in the posterior part of L (Fig. 12 - left; asterisks), while the anterograde labeling in the same case was rather dense. In contrast to that, DY injection in D6 caused retrograde labeling of numerous cells in L and Bp amygdaloid nuclei (Fig. 15A-D). This may suggest that FR is not the best retrograde marker and did not visualize all cells sending axons to the injection site. However, results of D6 appear to be representative to conclude that Sp is the cortex related to the lateral amygdaloid nucleus but preferentially to its middle (not pericapsular) sector. Such a distribution of labeled amygdaloid neurons, overlapping with terminals of the cortico-amygdaloid connections, supports the topography in L nucleus.

Injections into the dorsal Sylvian area have resulted in labeled cells appearing in the same amygdaloid nuclei Bm, Bp and L, as in case of Sp injections. The greatest number of labeled cells was found, however, in the basal magnocellular nucleus. In D7 (Fig. 7A-C; solid circles) and D11,R (Figs. 12A,B - right; asterisks and 14A) numerous labeled cells were predominantly accumulated in the dorsal part of Bm nucleus within the intermediate extent of the amygdala. The cells observed in the Bp and L nuclei were significantly less numerous in both cases.

Thus, the main difference in the arrangement of connections between the posterior and dorsal areas of the Sylvian gyrus is related to amygdaloid nuclei from which the most intense corticopetal projections originate. The posterior Sylvian area seems to be an extension of the cortical zone involving ventral EP and CP areas which are preferentially related to the lateral amygdaloid nucleus. In contrast, the dorsal Sylvian area is characterized by the most substantial projection originating from the basal magnocellular amygdaloid nucleus.

The amygdalofugal projection reaching the anterior Sylvian area appeared to be rather small and is illustrated by the FB injection in D7 (Sa; Figs. 3 and 7A-E; solid triangles). A few labeled cells were sparsely distributed through the Bp, Bm and anterodorsal part of L. Labeling of cells in the L can be produced by additional injection point in the Sp area on the opposite wall of the Sylvian gyrus.

DISCUSSION

The present study was undertaken to clarify the relations between the canine temporal neocortex and nuclei of the amygdaloid complex. It was found that only some temporal areas are connected with the amygdala, and that their connectivity patterns differ. The anterior ectosylvian (EA) area does not send or receive any amygdaloid projections. The middle ectosylvian (EM) and dorsal part of the posterior ectosylvian (EP) areas, as well as the anterior Sylvian (Sa) gyrus, have weak connections with the amygdala, whereas the ventral region of the temporal neocortex, including ventral EP, composite posterior (CP) and posterior Sylvian (Sp) gyri, is characterized by strong reciprocal connections with the -amygdaloid complex. A distinctive feature of cortico-amygdaloid connections (Fig. 16, upper scheme) is their preferential relation to the lateral sector of the lateral amygdaloid nucleus, whereas the most striking in distribution of amygdalo-cortical connections (Fig. 16, bottom scheme) is a substantial projection from the basal

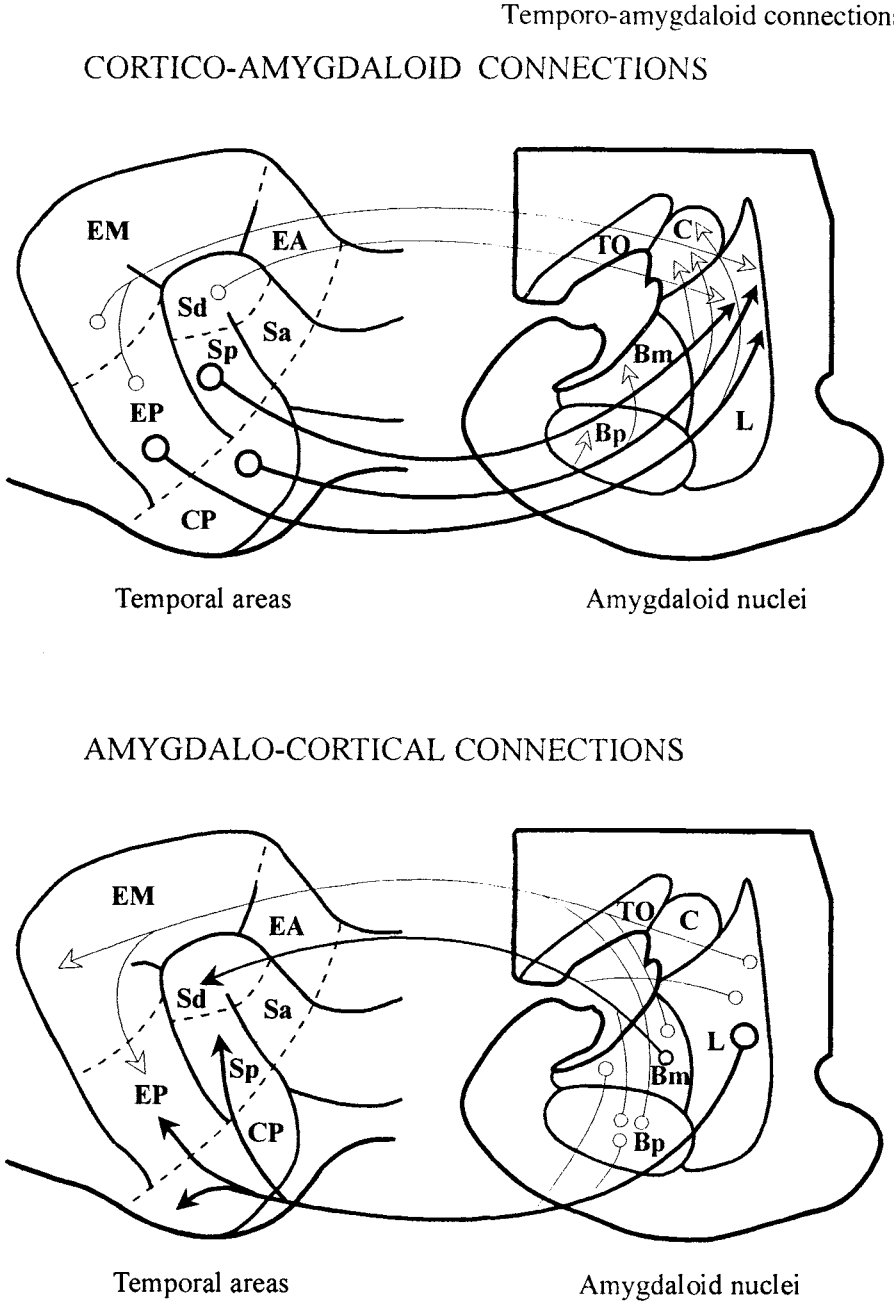

Fig. 16. Diagrammatic summary of cortico-amygdaloid and amygdalo-cortical connections between areas of the temporal cortex and amygdaloid nuclei are illustrated on the scheme of cortical surface (left) and coronal sections through the amygdala (right). Origin of projections is marked by open circles and places of their terminations by arrowheads. The density of projections is indicated by arrow thickness. See list of abbreviations for the nomenclature of subdivisions of the temporal cortex and amygdaloid nuclei.

magnocellular nucleus to the dorsal part of the Sylvian gyrus.

The cortical origin of amygdalopetal projections

In the dog, the cortex sending the most significant connections to the amygdala involves a large extent of neocortex located in the posterior composite (CP) gyrus, the posterior part of the Sylvian gyrus (Sp) and, additionally, the ventral part of area EP adjoining the CP. The amygdalopetal projection taking rise from the dorsal part of area EP is substantially less intense and diminishes in the direction of the middle ectosylvian area (EM). After injections in the area EM we were able to follow only single labeled axons in the amygdala. Thus, the amygdalopetal projection successively increases from the primary auditory cortex of the area EM, along area EP, towards the area CP and Sp.

In primates, the temporal neocortex in which the amygdalopetal projections take rise involves the anterior parts of the superior and inferior temporal gyri considered to be the association areas of the auditory and visual modalities, respectively (Turner et al. 1980, Iwai and Yukie 1987, Amaral et al. 1992, Baizer et al. 1993), as well as from the multimodal cortex of the superior temporal sulcus and temporal pole (Markowitsch et al. 1985, Moran et al. 1987). The auditory associative areas of the superior temporal gyrus in rhesus monkey have been identified as those sending amygdalopetal projections which gradually increase in intensity toward the polymodal temporopolar cortex (Kosmal et al. 1997). Thus, an open question remains whether in subprimates the cortex sending substantial projections to the amygdala constitutes unimodal or multimodal fields. Studies in the rat have shown that, in addition to projections deriving from the allo- and mesocortical regions (Ottersen 1982), the amygdalopetal projection originates from the temporal neocortical fields surrounding TE1 area (primary auditory field) considered to be auditory association fields (Mascagni et al. 1993, Romanski and LeDoux 1993a). In the cat, the temporal cortex sending projections to the amygdala is situated along and above the posterior and a small part of the anterior rhinal sulcus (area 36) as well as in the ventral most regions of the posterior Sylvian and posterior ectosylvian gyri (Russchen 1982, Shinonaga et al. 1994). The cortex was named "temporal polar" (Shinonaga et al. 1994), which suggests its correspondence to the cortex of the simian temporal pole, and it may also suggest a multimodal character of this cortex. In the dog, after injections into areas EP and CP we have found retrogradely labeled cells mainly in the dorsally adjacent auditory cortex. It seems that neurons of these areas form only short intracortical connections. This would suggest that the areas EP and CP constitute unimodal rather than multimodal auditory associative fields (personal observations). Their hierarchy should be determined, however, by examination of the laminar organization of intracortical connections.

Terminal distribution of the cortico-amygdaloid connections

The corticofugal projection originating from the ectosylvian, posterior composite and posterior Sylvian gyri in the dog terminate predominantly in the lateral nucleus of the amygdala. Less dense axonal terminals have been observed in the lateral part of the central and both basal nuclei (Fig. 16, upper scheme).

The most distinctive feature of this cortico-amygdaloid projection is dense terminations of neocortical axons in the lateral sector of the lateral nucleus, together with its dorsal tip situated between fibers of external capsule and putamen. Axonal terminals overlap the population of pericapsular, deeply Nissl-stained neurons forming a characteristic cytoarchitectonic picture of the lateral nucleus in the carnivore (Kosmal and Nitecka 1977, Krettek and Price 1978). In the early myeloarchitectonic descriptions of the canine amygdaloid complex this dorsal tip of the lateral nucleus was, however, distinguished as "nucleus putaminalis" (Maksymowicz 1963, Miodonski 1965). Our data showing the arrangement of both anterograde and retrograde labeling, particularly dense in the most dorsal tip of the lateral nucleus, give evidence that the whole lateral region constitutes an integral sector of the lateral nucleus. This suggestion is in agreement with data obtained in the cat by Smith and Pare (1994). They have distinguished two sectors in the lateral nucleus, each having different intra-amygdaloid connections: lateral (pericapsular or shell) and medial (core). The lateral sector of the lateral nucleus projected to the basolateral, whereas the medial sector projected to the basomedial amygdaloid nucleus. Besides cytoarchitectonic evidence, our study provides connectional data, supporting the view about internal differentiation of the lateral nucleus. We observed the latero-medial topography of amygdalopetal projections. In accordance to that the pericapsular part of the nucleus was predominantly related to the ventral EP and CP, whereas the intermediate nucleus part was related to the area Sp.

Thus the projection taking rise in the posterior Sylvian cortex seems to be an extension of that arising from the posterior composite gyrus. Such topography of the projection supports data obtained in the cat, where the posterior Sylvian cortex is considered to be the temporal part of the gyrus in contrast to its anterior, insular part (Cranford et al. 1976).

In primates, the cortico-amygdaloid projections originate from the superior and inferior parts of the temporal gyrus and terminate in both the lateral and basal amygdaloid nuclei (Herzog and Van Hoesen 1976, Aggleton et al. 1980, Amaral and Price 1984, Amaral et al. 1992). The superior temporal gyrus, however, is reciprocally connected with the lateral nucleus, whereas the inferotemporal cortex is reciprocally connected with the basal

lateral nucleus (Iwai and Yukie 1987, Baizer et al. 1993). The difference in distribution of temporo-amygdaloid connections in monkey reflects the specificity of the functional organization of the temporal cortex. The superior temporal cortex involves associative areas related to the auditory modality while the inferotemporal cortex relates to vision (Chavis and Pandya 1976, Turner et al. 1980, Pandya and Yeterian 1985, Iwai and Yukie 1987, Weller and Steele 1992). Thus, taking into account that, in the dog, projections originating from the areas EP and CP terminate in the similar part of the lateral amygdaloid nucleus as the projection of the superior temporal gyrus in the monkey, it may be suggested that areas EP and CP are equivalent to the auditory association cortex of the monkey.

As mentioned above, we have also observed a corticofugal projection directed to the lateral part of the central nucleus. Previous cytoarchitectonic, immunocytochemical and connectivity studies, especially numerous in the rat, have revealed that the central nucleus can be divided into several subdivisions (McDonald 1982, 1992, DeOlmos et al. 1985, Cassell et al. 1986, Cassell and Gray 1989, Mascagni et al. 1993, Romanski and LeDoux 1993b). The number of subdivisions depends on the techniques applied and on the criterion used for parcellation. In all investigated species, however, the medial and lateral subdivisions of the central nucleus have been distinguished. The central lateral nucleus in the cat, as in the dog, occupies the dorsolateral part of the amygdala, where it merges with the putamen (Krettek and Price 1978). The border between these two structures is rather difficult to delineate due to their cytoarchitectonic and AChE- chemoarchitectonic similarity (high level of AChE staining) and, therefore, the lateral part of the central amygdaloid nucleus is often considered as a transitional amygdalo-striatal region (DeOlmos et al. 1985). Contrary to that, the central lateral nucleus of the monkey was found to have lighter AChE staining than either the putamen or the medial division of the central nucleus (Amaral and Bassett 1989). It is unclear whether these discrepancies are related to different nomenclature of particular subdivisions of the nucleus or if they reflect the structural differences between the primate and nonprimate central amygdaloid nucleus.

In the dog, we found that corticofugal projections directed into the lateral part of the central nucleus and the putamen formed separate systems of fibers. The terminals of connections reaching the putamen were localized more dorsally in comparison with those found in the central nucleus (personal observations). These results are in agreement with recent data in the rat where regions of the central nucleus placed ventrally to the putamen are recognized as a target of corticofugal connections originating in the auditory association areas of the temporal neocortex (Mascagni et al. 1993, Romanski and LeDoux 1993b).

In the dog, basal amygdaloid nuclei received a less substantial projection from the temporal cortex, mainly from the area CP. Among the basal nuclei only single axons were seen in the Bm, whereas a more profuse projection, formed by extremely thin axons, was directed to the small central area of Bp nucleus. This result is in contrast to that in the cat where corticofugal connections are rather directed to the basolateral amygdaloid nucleus (Russchen 1982). A projection terminating in the basomedial nuclei in addition to the other amygdaloid nuclei was, however, observed in the rat. Its origin was identified in the neurons of agranular insular and perirhinal cortices. Their axons reach a large amygdaloid region involving the lateral, basolateral and basomedial nuclei (McDonald and Jackson 1987). In the macaque monkey, the basal nuclei are a target of significant corticofugal projections, taking rise from the unimodal association areas and polymodal fields of the temporal cortex. They terminate in both basal and accessory basal nuclei (Markowitsch et al. 1985, Iwai and Yukie 1987, Moran et al. 1987, Amaral et al. 1992, Baizer et al. 1993).

Amygdalofugal projections to the temporal neocortex and reciprocity of connections

Three amygdaloid nuclei, the lateral, basal magnocellular and basal parvocellular, project to the canine temporal neocortex (Fig. 16, bottom scheme). Amygdalo-cortical axons spread into the whole temporal cortex, with the exception of area EA. The most distinctive are connections arising from the dorsolateral - pericapsular and caudal parts of the lateral nucleus of the amygdala reaching the areas of the posterior composite and posterior ectosylvian gyri as well as connections from the basal magnocellular nucleus terminating in the dorsal part of the Sylvian gyrus.

A projection deriving from the pericapsular part of the lateral nucleus was previously defined in the dog in a study applying anterograde degeneration methods. It showed that degenerated amygdalo-cortical fibers were more plentiful if the lesion involved the pericapsular region of the lateral nucleus (Kosmal 1976). Results in the

dog are also in agreement with data obtained in other mammals where the lateral nucleus is a source of substantial corticopetal connections. In the monkey, the dorsolateral part of the lateral amygdaloid nucleus seems to be especially related to the temporal auditory association fields, however, amygdalofugal projection, besides the ventral region of the temporal cortex, extends into the insular, medial and caudal orbital as well as occipital cortex (Amaral and Price 1984, Amaral et al. 1992, Kosmal et al[.] 1997). McDonald and Jackson (1987) have found, in the rat, that the neocortex situated dorsally to the prorhinal area 36 receives a substantial projection from the posterodorsal part of the lateral nucleus. This projection seems to be reciprocal because the lateral nucleus receives an intense, topographically organized amygdalopetal projection (Mascagni et al. 1993, Romanski and LeDoux 1993b). The reciprocity of connections in the dog was manifested in our material by overlapping localization of retrogradely labeled cells and anterograde labeling of axonal terminals which was especially clear in the pericapsular part of the lateral amygdaloid nucleus.

We observed that less substantial but widespread amygdalo-cortical projections originate from the basal amygdaloid nuclei. In the dog, a weak projection from both basal nuclei was directed to almost the entire extent of the temporal cortex, however, connections from the basal magnocellular nucleus seemed to be focused in the dorsal Sylvian gyrus. Moreover, this projection shows less significant reciprocity because connections in the opposite direction seem to be much weaker. The results obtained in various species suggest that the basal lateral nucleus should be considered an output nucleus to a large neocortical region. In the cat (Macchi et al. 1978, Sripanidkulchai et al. 1984, Llamas et al. 1985) the projections from the basal lateral nucleus are directed to wide areas of the frontal, cingular, insular Sylvian and somatosensory cortices, which are in turn a source of cortico-amygdaloid projections terminating in the basal lateral nucleus (Russchen et al. 1982, DeOlmos et al. 1985).

A review of data obtained in other species suggests that the basal magnocellular nucleus is the amygdaloid structure modifying the incoming information which is next directed into wide neocortical areas. It has also been shown that the basal nuclei are the site of extensive convergence of sensory information (Knuepfer et al. 1995) which may reach the nucleus directly or through the intra-amygdaloid connections from the lateral nucleus (Amaral et al 1992, Romanski et al. 1993, Smith and Pare 1994, Pitkanen et al. 1995). Additionally, the basal amygdaloid nuclei are sites of convergence of projections arising from structures of various functional attributes such as hippocampus, medial geniculate or basal forebrain (Mello et al. 1992a,b). The great complexity of the amygdalopetal connections may suggest that in the amygdaloid complex exteroceptive and interoceptive signals undergo processes of modulation (Knuepfer et al. 1995).

ACKNOWLEDGEMENTS

The authors thank Prof. K. Zieliński, dr R. Saunders and Prof. W. Kozak for helpful comments and criticism. We also thank Ms. D. Borkowska, T. Cymbalak and E. Krasnodębska for technical assistance. This research was supported by the State Committee for Scientific Research (KBN) grant 6 6330 9203 p/02.

ABBREVIATIONS

Bm - basal magnocellular nucleus of the amygdala
Bp - basal parvicellular nucleus of the amygdala
C - central nucleus of the amygdala
CE - entorhinal cortex
Ci - central nucleus, intermediate division
Cl - central nucleus, lateral division
Cm - central nucleus, medial division
Co - cortical nucleus of the amygdala
CP - posterior composite area
CPr - periamygdaloid cortex
Cr - cruciate sulcus
EA - ectosylvian gyrus, anterior area
EM - ectosylvian gyrus, middle area
EP - ectosylvian gyrus, posterior area
ES - ectosylvian sulcus
H - hippocampus
L - lateral nucleus of the amygdala
LS - lateral sulcus
M - medial nucleus of the amygdala
PS - presylvian sulcus
Rha - anterior rhinal sulcus
Rhp - posterior rhinal sulcus
S - Sylvian sulcus
Sa - Sylvian gyrus, anterior division
Sd - Sylvian gyrus, dorsal division
Sp - Sylvian gyrus, posterior division
SS - suprasylvian sulcus
TO - optic tract

REFERENCES

Adams J.C. (1981) Heavy metal intensification of DAB - based HRP reaction product. J. Histochem. Cytochem. 6: 775

Aggleton J.P. (1993) The contribution of the amygdala to normal and abnormal emotions states. TINS 16: 328-333.

Aggleton J.P., Burton M.J., Passingham R.E. (1980) Cortical and subcortical afferents to the amygdala of the rhesus monkey (Macaca mulatta). Brain Res. 190: 347-368.

Aggleton J.P., Mishkin M. (1986) The amygdala: sensory gateway to the emotions. In:Emotion: theory, research, and experience (Eds. R.A. Plutchik and H. Kellerman). Orlando, Academic Press, p. 281-299.

Amaral D.G., Bassett J.L. (1989) Cholinergic innervation of monkey amygdala: an immunohistochemical analysis with antisera to choline acetyltransferase. J. Comp. Neurol. 281: 337-361.

Amaral D.G., Price J.L. (1984) Amygdalo-cortical projections in the monkey (Macaca fascicularis). J. Comp. Neurol. 230: 465-496.

Amaral D.G., Price J.L., Pitkanen A., Carmichael S.T. (1992) Anatomical organization of the primate amygdaloid complex. In: The amygdala: neurobiological aspects of emotion, memory and mental dysfunction (Ed. J.P. Aggleton). Wiley, New York, p. 1-66.

Baizer J.S., Desimone R., Ungerleider L.G. (1993) Comparison of subcortical connections of inferior temporal and posterior parietal cortex in monkeys. Visual Neurosci. 10: 59-72.

Brandt H.M., Apkarian A.V. (1992) Biotin-dextran: a sensitive anterograde tracer for neuroanatomic studies in rat and monkey. J. Neurosci. Methods 45: 35-40.

Cassell M.D., Gray T.S. (1989) Morphology of peptide-immunoreactive neurons in the rat central nucleus of the amygdala. J. Comp. Neurol. 281: 320-333.

Cassell M.D., Gray T.S., Kiss J.Z. (1986) Neuronal architecture in the rat central nucleus of the amygdala: a cytological, hodological, and immunocytochemical study. J. Comp. Neurol. 246: 478-499.

Chavis D.A., Pandya D.N. (1976) Further observations on corticofrontal connections in the rhesus monkey. Brain Res. 117: 369-386.

Cranford J.L., Ladner S.J., Cambpell C.B.G., Neff W.D. (1976) Efferent projections of the insular and temporal neocortex of the cat. Brain Res. 117:195-210.

DeOlmos J.S., Alheid G.F., Beltramino C.A. (1985) Amygdala. In: The rat nervous system (Ed.G. Paxinos). Orlando, Academic Press, p. 223-334.

Geneser-Jensen F.A., Blackstad T.W. (1971) Distribution of acetylcholinesterase in the hippocampal region of the guinea pig. I. Entorhinal area, parasubiculum, and presubiculum. Z. Zellforsch. 114: 460-481.

Herzog A., Van Hoesen G.W. (1976) Temporal neocortical afferent connections to the amygdala in the rhesus monkey. Brain Res. 115: 57-69.

Iwai E., Yukie M. (1987) Amygdalofugal and amygdalopetal connections with modality-specific visual cortical areas in macaques (Macaca fuscata, M. mulatta, and M. fascicularis). J. Comp. Neurol. 261: 362-387.

Kesner R.P. (1992) Learning and memory in rats with an emphasis on the role of the amygdala. In: The amygdala: neurobiological aspects of emotion, memory and mental dysfunction (Ed.J.P. Aggleton). Wiley, New York, p. 379-399.

Kisvarday Z.F., Beaulieu C., Eysel U.T. (1993) Network of GABAergic large basket cells in cat visual cortex (area 18): implication for lateral disinhibition. J. Comp. Neurol. 327: 398-415.

Knuepfer M.M., Eismann A., Schutze I., Stumpf H., Stock G. (1995) Responses of single neurons in amygdala to interoceptive and exteroceptive stimuli in conscious cats. Am. J. Physiol. 268: 666-675.

Kosmal A. (1976) Efferent connections of the basolateral amygdaloid part to the archi-, paleo-, and neocortex in dogs. Acta Neurobiol. Exp. 36: 319-331.

Kosmal A., Malinowska M., Kowalska D.M. (1997) Thalamic and amygdaloid connections of the auditory association cortex of the superior temporal gyrus in rhesus monkey (Macaca mulatta). Acta Neurobiol. Exp. 57: 165-188.

Kosmal A., Nitecka L. (1977) Cytoarchitecture and acetylcholinesterase activity of the amygdaloid nuclei in the dog. Acta Neurobiol. Exp. 37: 363-374.

Kreiner J. (1966) Reconstruction of neocortical lesions within the dog's brain: instructions. Acta Biol. Exp. 26: 221-243.

Krettek J.E., Price J.L. (1978) A description of the amygdaloid complex in the rat and cat with observations on intra-amygdaloid axonal connections. J. Comp. Neurol. 178: 255-280.

LeDoux J.E. (1992) Emotion and the amygdala. In: The amygdala: neurobiological aspects of emotion, memory and mental dysfunction (Ed. J.P. Aggleton). Wiley, New York, p. 339-351.

Llamas A., Avendano C., Reinoso-Suarez F. (1985) Amygdaloid projections to the motor, premotor and prefrontal areas of the cat's cerebral cortex: a topographical study using retrograde transport of horseradish peroxidase. Neuroscience 15: 651-657.

Macchi G., Bentivoglio M., Rossini P., Tempesta E. (1978) The basolateral amygdaloid projections to the neocortex in the cat. Neurosci. Lett. 9: 347-351.

Maksymowicz K. (1963) The amygdaloid complex of the dog. Acta Biol. Exper. 23: 63-73.

Markowitsch H.J., Emmans D., Irle E., Streicher M., Preilowski B. (1985) Cortical and subcorticalafferent connections of the primate's temporal pole: a study of rhesus monkeys, squirrel monkeys, and marmosets. J. Comp. Neurol. 242: 425-458.

Mascagni F., McDonald A.J., Coleman J.R. (1993) Corticoamygdaloid and corticocortical projections of the rat

temporal cortex: a Phaseolus vulgaris leucoagglutinin study. Neuroscience 57: 697-715.

McDonald A.J. (1982) Cytoarchitecture of the central amygdaloid nucleus of the rat. J. Comp. Neurol. 208: 401-418.

McDonald A.J. (1992) Cell types and intrinsic connections of the amygdala. In: The amygdala: neurobiological aspects of emotion, memory and mental dysfunction (Ed. J.P. Aggleton). Wiley, New York, p. 67-96.

McDonald A.J., Jackson T.R. (1987) Amygdaloid connections with posterior insular and temporal cortical areas in the rat. J. Comp. Neurol. 262: 59-77.

Mello L.E., Tan A.M., Finch D.M. (1992a) Convergence of projection from the rat hippocampal formation, medial geniculate and basal forebrain onto single amygdaloid neurons: an in vivo extra- and intracellular electrophysiological study. Brain Res. 587: 24-40.

Mello L.E., Tan A.M., Finch D.M. (1992b) GABAergic synaptic transmission in projections from the basal forebrain and hippocampal formation to the amygdala: an in vivo iontophoretic study. Brain Res. 587: 41-48.

Miodonski R. (1965) Myeloarchitectonics of the amygdaloid complex of the dog. Acta Biol. Exper. 4: 263-287.

Moran M.A., Mufson E.J., Mesulam M.M. (1987) Neural inputs into the temporopolar cortex of the rhesus monkey. J. Comp. Neurol. 256: 88-103.

Murray E.A. (1992) Medial temporal lobe structures contributing to recognition memory: the amygdaloid complex versus the rhinal cortex. In: The amygdala: neurobiological aspects of emotion, memory and mental dysfunction (Ed. J.P. Aggleton). Wiley, New York, p. 453-470.

Ottersen O.P. (1982) Connections of the amygdala of the rat. IV: corticoamygdaloid and intraamygdaloid connections as studied with axonal transport of horseradish peroxidase. J. Comp. Neurol. 205: 30-48.

Pandya D.N., Yeterian E.H. (1985) Architecture and connections of cortical association areas. In: Cerebral cortex: association and auditory cortices (Eds. A. Peters and E.G. Jones). Plenum Press, New York, p. 3-61.

Pitkanen A., Stefanacci L., Farb C.R., Genevieve Go G., LeDoux J.E., Amaral D.G. (1995) Intrinsic connections of the rat amygdaloid complex: projections originating in the lateral nucleus. J. Comp. Neurol. 356: 288-310.

Rolls E.T. (1992) Neurophysiology and functions of the primate amygdala. In: The amygdala: neurobiological aspects of emotion, memory and mental dysfunction (Ed. J.P. Aggleton). Wiley, New York, p. 143-165.

Romanski L.M., Clugent M.C., Bordi F., LeDoux J.E. (1993) Somatosensory and auditory convergence in the lateral nucleus of the amygdala. Behav. Neurosci. 107: 444-450.

Romanski L.M., LeDoux J.E. (1993a) Organization of rodent auditory cortex: anterograde transport of PHA-L from MGv to temporal neocortex. Cerebral Cortex 3: 499-514.

Romanski L.M., LeDoux J.E. (1993b) Information cascade from primary auditory cortex to the amygdala: corticocortical and corticoamygdaloid projections of temporal cortex in the rat. Cerebral Cortex 3: 515-532.

Rosene D.L., Roy N.J., Davis B.J. (1986) A cryoprotection method that facilitates cutting frozen sections of whole monkey brains for histological and histochemical processing without freezing artifact. J. Histochem. Cytochem. 34(10): 1301-1315.

Russchen F.T. (1982) Amygdalopetal projections in the cat. I. Cortical afferent connections. A study with retrograde and anterograde tracing techniques. J. Comp. Neurol. 206: 159-179.

Shinonaga Y., Takada M., Mizuno N. (1994) Direct projections from the non-laminated division of the medial geniculate nucleus to the temporal polar cortex and amygdala in the cat. J. Comp. Neurol. 340: 405-426.

Smith Y., Pare D. (1994) Intra-amygdaloid projections of the lateral nucleus in the cat: PHA-L anterograde labeling combined with postembedding GABA and glutamate immunocytochemistry. J. Comp. Neurol. 342: 232-248.

Sripanidkulchai K., Sripanidkulchai B., Wyss J.M. (1984) The cortical projection of the basolateral amygdaloid nucleus in the rat: a retrograde fluorescent dye study. J. Comp. Neurol. 229: 419-431.

Sychowa B. (1963) Degeneration of the medial geniculate body following ablations of various temporal regions in the dog. Acta Biol. Exp. 23: 75-99.

Totterdell S., Ingham C.A., Bolam J.P. (1992) Immunocytochemistry I: pre-embedding staining. In: Experimental neuroanatomy (Ed. J.P. Bolam). Oxford University Press, New York, p. 103-127.

Tunturi A.R. (1950) Physiological determination of the boundary of the acoustic area in the cerebral cortex of the dog. Am. J. Physiol. 160: 395-401.

Tunturi A.R. (1962) Frequency arrangement in anterior ectosylvian auditory cortex of dog. Am. J. Physiol. 203: 185-193.

Tunturi A.R. (1970) The pathway from the medial geniculate body to the ectosylvian auditory cortex in the dog. J. Comp. Neurol. 138: 131-136.

Turner B.H., Mishkin M., Knapp M. (1980) Organization of the amygdalopetal projections from modality-specific cortical association areas in the monkey. J. Comp. Neurol. 191: 515- 543.

Van Hoesen G. (1981) The differential distribution, diversity and sprouting of cortical projections to the amygdala in the rhesus monkey. In: The amygdaloid complex (Ed. Y. Ben-Ari). North-Holland Biomedical Press, Elselvier, Amsterdam, p. 77-89.

Veenman C.L., Reiner A., Honig M.G. (1992) Biotinylated dextran amine as an anterograde tracer for single- and double-labeling studies. J. Neurosci. Methods 41: 239-254.

Weller R.E., Steele G.E. (1992) Cortical connections of subdivisions of inferior temporal cortex in squirrel monkeys. J. Comp. Neurol. 324: 37-66.

Received 4 July 1997, accepted 21 October 1997